Energy Materials and Devices

Review

Challenges and opportunities facing zinc anodes for aqueous zinc-ion battery

Boyu Li, Yuetao Ma, Jiabin Ma, Likun Chen, Yang Zhao, and Man-Chung Tang ✉

Graphical Abstract

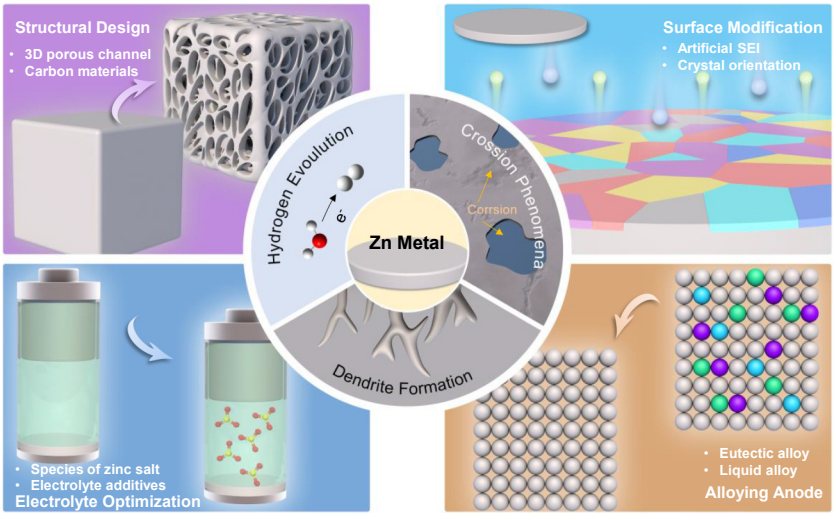

This review introduces the challenges and optimization strategies of zinc metal anode for aqueous zinc-ion batteries. In addition, the development prospects for new configuration zinc metal anode are proposed.

✉Address correspondence to Man-Chung Tang, Kobetang2021@sz.tsinghua.edu.cn

Received: August 16, 2024
Accepted: September 2, 2024

Read Online

Submit Online

Citation: Li B., Ma Y., Ma J., et al. Challenges and opportunities facing zinc anodes for aqueous zinc-ion battery. *Energy Mater. Devices*, 2024, 2(3), 9370044. https://doi.org/10.26599/EMD.2024.9370044

Energy Materials and Devices

Open Access

Review

https://doi.org/10.26599/EMD.2024.9370044

Challenges and opportunities facing zinc anodes for aqueous zinc-ion battery

Boyu Li[1,2,†], Yuetao Ma[1,2,†], Jiabin Ma[1,2], Likun Chen[1,2], Yang Zhao[1,2], and Man-Chung Tang[1] ✉

[1] *Shenzhen All-Solid-State Lithium Battery Electrolyte Engineering Research Center, Institute of Materials Research (IMR), Tsinghua Shenzhen International Graduate School, Shenzhen 518055, China*

[2] *School of Materials Science and Engineering, Tsinghua University, Beijing 100084, China*

[†] *Boyu Li and Yuetao Ma contributed equally to this work.*

Received: August 16, 2024 / **Accepted:** September 2, 2024

ABSTRACT

Rechargeable aqueous zinc-ion batteries (ZIBs) have gained attention as promising candidates for next-generation large-scale energy storage systems due to their advantages of improved safety, environmental sustainability, and low cost. However, the zinc metal anode in aqueous ZIBs faces critical challenges, including dendrite growth, hydrogen evolution reactions, and corrosion, which severely compromise Coulombic efficiency and cycling stability, hindering their broader adoption. This review first explores the fundamental mechanisms underlying these challenges and then examines current strategies to address them, focusing on structural design, surface modifications, electrolyte optimization, and alloying treatments. Finally, potential future directions are discussed, outlining a pathway toward achieving high-performance aqueous ZIBs.

KEYWORDS

aqueous zinc-ion batteries, zinc metal anode, structural design, surface modification, electrolyte optimization, alloying anode

1 Introduction

The utilization of fossil fuels has played a pivotal role in driving the rapid progress of human civilization. However, it has also introduced significant environmental challenges that require urgent resolution. To achieve sustainable development, the adoption of clean, pollution-free secondary energy sources, such as wind and solar power, has emerged as a critical future trend[1–5]. Despite their potential, the direct storage and utilization of these energy sources present considerable challenges. Electrical energy, serving as an intermediary between energy harvesting and utilization, offers an effective solution. Consequently, the development of high-efficiency electrical energy storage systems (EESs) is essential for supporting humanity's sustainable growth. In recent years, secondary batteries, as a key type of EES, have gained prominence due to their resource efficiency and environmental benefits. They have become integral to modern life, powering devices such as mobile phones, laptops, and electric vehicles[6–8].

Among these, lithium-ion batteries (LIBs) dominate the energy storage market, owing to their high energy density, elevated output voltage, and long cycle life[9–11]. However, due to the high electrochemical reactivity of lithium, most LIBs rely on costly organic electrolytes. While organic electrolytes offer a wide electrochemical window and relative stability, they suffer from drawbacks such as high toxicity, cost, and flammability, which hinder their broader application[7,12–14]. In the realm of large-scale energy storage, aqueous electrolyte battery systems have gained significant attention[15]. Compared to traditional organic electrolytes, aqueous electrolytes offer two orders of magnitude higher ion conductivity (~1 S cm^{-2}) and are more cost-effective, environmentally friendly, and safer[16,17].

Historically, zinc metal has been extensively used

✉ Address correspondence to Man-Chung Tang, Kobetang2021@sz.tsinghua.edu.cn

in dry batteries, such as zinc–manganese (Zn/MnO_2), zinc–nickel (Zn/NiOOH), and zinc–silver (Zn/AgO) systems[18–20]. However, dry batteries present challenges, including high toxicity, disposal difficulties, and environmental pollution, leading to a decline in their development[21]. In 1986, Yamamoto et al.[22] introduced the $Zn|ZnSO4|MnO_2$ battery system, replacing organic electrolytes with zinc salt solutions. Although this system was unstable and had a short cycle life, it marked the inception of zinc-ion batteries (ZIBs). Recently, aqueous ZIBs have rapidly advanced among rechargeable aqueous batteries. Zinc metal is particularly suited for use with aqueous electrolytes, as its stable equilibrium potential (Zn^{2+}/Zn at −0.76 V vs. the standard hydrogen electrode [SHE]) prevents violent reactions with water. Furthermore, zinc offers a high theoretical specific gravimetric capacity (820 mAh g^{-1}) and a high specific volumetric capacity (5855 mAh cm^{-3}) due to the redox process involving two electrons per zinc atom. Zinc also benefits from being low-cost, low-toxicity, environmentally benign, and resource-abundant[23–25]. In addition, the typical layered cathode materials, such as manganese and vanadium oxides, offer high theoretical capacity at a low cost, making ZIBs an attractive option for aqueous electrolyte systems. As a result, aqueous ZIBs have garnered substantial attention from researchers.

Taking manganese-based aqueous ZIBs as an example, the reaction mechanism of aqueous ZIBs can be illustrated through the charge and discharge processes. During these processes, zinc ions migrate between the anode and cathode, while an equivalent current flows through the external circuit[26,27]. At the anode, zinc ions undergo reversible stripping and plating, and at the cathode, zinc ions are intercalated into and deintercalated from the cathode materials[28,29]. The corresponding electrode reactions are as follows:

Anode reaction: $Zn = Zn^{2+} + 2e^-$

Cathode reaction: $Zn^{2+} + 2e^- + 2MnO_2 = ZnMn_2O_4$

Overall reaction: $Zn + 2MnO_2 = ZnMn_2O_4$

The underlying mechanism of ZIBs primarily involves the disproportionation and neutralization reactions among Mn^{4+}, Mn^{3+}, and Mn^{2+}.

Compared to commercial LIBs, aqueous ZIBs offer several notable advantages:

1. **Low cost.** Zinc metal is abundant and easy to purify, making it one of the most inexpensive metals. In addition, ZIBs can be fabricated under ambient conditions, reducing manufacturing costs significantly. The use of aqueous electrolytes instead of costly organic solutions further enhances cost efficiency, making ZIBs a promising option for large-scale energy storage[30,31].

2. **High power density.** Rapid charge and discharge are critical in practical applications. Due to the fast ion conduction in aqueous electrolytes, the power density of aqueous ZIBs can reach up to 12 kW kg^{-1}, nearly equivalent to the power density of supercapacitors, which are known for their excellent power delivery[32].

3. **High safety and environmental benignity.** Zinc salt-based aqueous electrolytes are non-toxic, recyclable, non-flammable, and environmentally friendly. Zinc metal, known for its low toxicity, has the lowest oxidation-reduction potential among metals that can stably exist in water[33]. Moreover, well-established technologies for zinc production and recycling minimize environmental impact, making aqueous ZIBs a strong candidate for next-generation energy storage devices[34].

Initially, research on ZIBs focused on MnO_2-based cathode materials, aiming to enhance capacity and cyclability by identifying zinc-intercalated materials with large channels and stable structures. To address challenges such as material dissolution[35], structural degradation[29], electrostatic shielding[36], and the generation of by-products[37], researchers have developed various cathode materials, including manganese-based[38–40], vanadium-based[41–43], Prussian blue analogs[44,45], and organic complexes[37,46]. While progress has been made, persistent issues on the anode side continue to limit further advancements in aqueous ZIBs.

Compared to the cathode, research on the zinc metal anode is still in its early stages, with few comprehensive reviews on the challenges and solutions associated with using zinc as an anode in aqueous ZIBs. The zinc metal anode faces significant challenges, such as dendrite growth and side reactions, which undermine Coulombic efficiency, cycle life, and rate performance[47–49]. Although cathode modifications can enhance battery performance, the zinc anode's issues remain a critical limiting factor.

In this review, we first outline the problems associated with zinc metal anodes, examining the mechanisms behind dendrite growth, hydrogen evolution, and corrosion. We explain how these issues degrade the electrochemical performance of ZIBs. Next, we review the literature on modified zinc metal anodes, categorizing potential solutions into structural design, surface modification, electrolyte optimization, and alloying treatments. In addition, we evaluate the advantages and limitations of these approaches. Finally, we propose future perspectives for research on zinc metal anodes in aqueous ZIBs. Overall, this review aims to provide deeper insights into zinc anode mechanisms and optimizations, advancing the commercial application of aqueous ZIBs.

2 Issues facing zinc metal anode of ZIBs

2.1 Mechanism of dendrite formation

Uniform and dense metal deposition is crucial for the

electrochemical performance of batteries, directly influencing Coulombic efficiency and cycle life. However, in metal-based anode batteries, dendrite growth is inevitable due to the micro-scale unevenness of the electrode and small-scale variations in electrolyte concentration. The two main factors driving dendrite formation are the inhomogeneous electric field distribution caused by the non-uniform surface of the anode and fluctuations in electrolyte concentration near the anode[27,50].

Using alkaline aqueous electrolytes as an example (Fig. 1), zincates act as the charge carriers during the electrochemical deposition process[51]. Initially, zincates adsorb onto the electrode surface, preferentially reducing and accumulating at energetically favorable sites, which forms the initial small tip and triggers the "cusp effect". This effect concentrates the charge at the tip, attracting further zincate transport and deposition. However, during the electrochemical stripping process, zinc does not strip preferentially from the tip, leading the small cusps to evolve into dendrites after several cycles. These zinc dendrites grow perpendicularly to the anode surface, resulting in a loose, porous structure that increases internal resistance and compromises anode stability. In severe cases, dendrites may puncture the separator, causing micro-short circuits or detaching from the current collector to form "dead zinc"[52,53].

The dendrite formation mechanism in neutral electrolytes is similar to that in mildly acidic electrolytes[54]. Zinc ions adsorb onto the anode surface, undergo two-dimensional diffusion, and accumulate into initial cusps. These cusps exacerbate the electric field's inhomogeneity, causing zinc ions to continue accumulating at the tips, eventually forming dendrites over repeated cycles[55,56]. While zinc is less

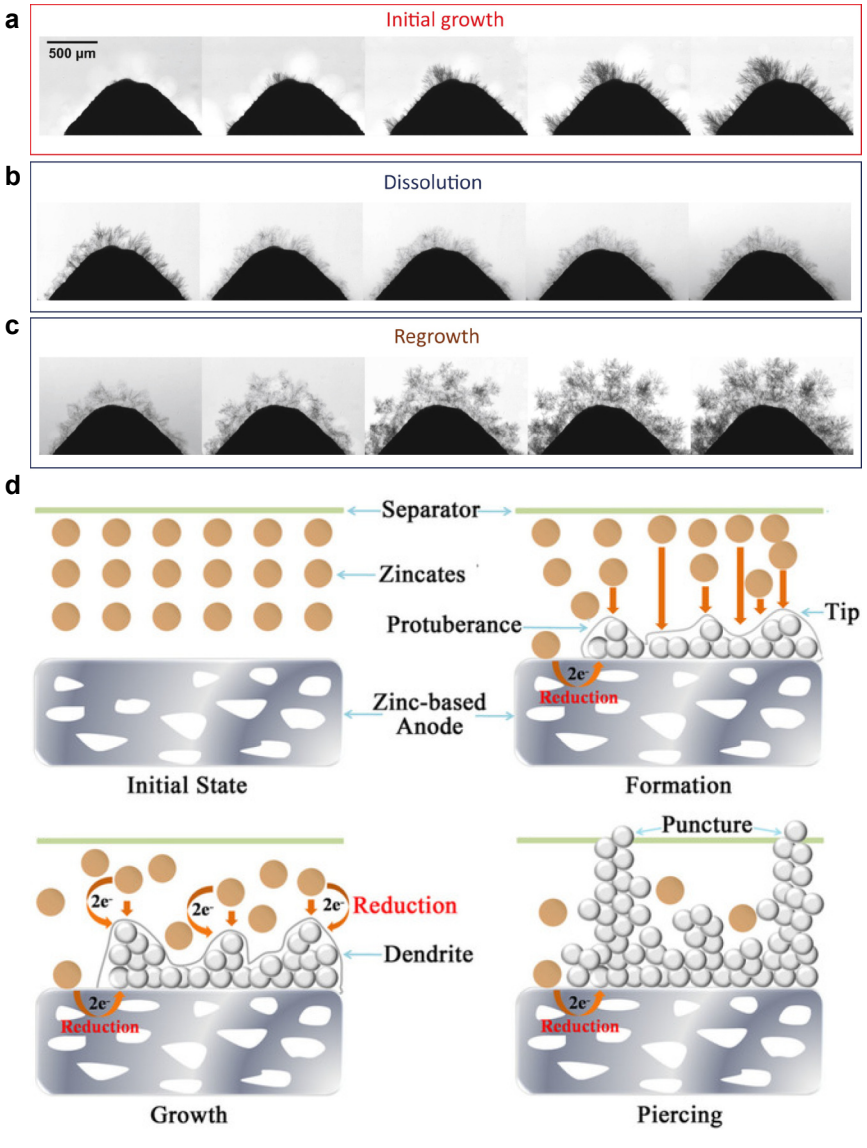

Figure 1 Operando study of zinc dendrites: growth (a), dissolution(b), and regrowth (c). Reproduced with permission from Ref. [53] ©2018, Elsevier Inc. (d) Mechanism of zinc dendrite formation in alkaline electrolytes. Reproduced with permission from Ref. [52] ©2018, Wiley-VCH Verlag GmbH & Co. KGaA, Weinheim.

likely to form a dense, insulative passivation layer that would increase internal resistance[57,58], the high Young's modulus of zinc makes its dendrites prone to rapid penetration, potentially resulting in micro-short circuits in ZIBs[59]. Although dendrite growth is somewhat mitigated in neutral and mildly acidic electrolytes due to higher overpotential[60], it remains a significant factor contributing to the poor electrochemical performance of ZIBs[61].

2.2 Hydrogen evolution reaction

This self-corrosion leads to the production of hydrogen gas, a process known as the hydrogen evolution reaction (HER). Compared to LIBs using organic electrolytes, aqueous batteries are more prone to HER at the electrolyte/anode interface[62,63]. As shown in Fig. 2a, the equilibrium potential of Zn/Zn^{2+} is lower than that of H_2O/H_2 across the full pH range[64], indicating that HER proceeds thermodynamically and spontaneously, rendering zinc metal unstable in water. Consequently, the spontaneous generation of hydrogen gas and the reduction of water increase internal pressure within sealed systems and consume the electrolyte[65]. The self-corrosion phenomenon in aqueous ZIBs often occurs in mildly acidic aqueous electrolytes (Fig. 2b)[62].

In practical aqueous ZIBs, the HER process is influenced by both the thermodynamics and kinetics of the gas-liquid phase transition. During the charging process, the zinc deposition reaction competes with HER, which significantly reduces Coulombic efficiency and cycle stability. This also causes volume expansion and directly compromises battery safety[65,66].

In alkaline electrolytes, the reduction potential of hydrogen is −0.83 V, whereas the reduction potential of zinc is −1.26 V[67]. According to the principle that materials with higher reduction potentials tend to gain electrons more readily, the HER takes precedence (Eq. 1)[68].

$$2H_2O + 2e^- = H_2\uparrow + 2OH^- \quad (1)$$

In reality, the extent of HER in aqueous ZIBs is significantly lower than theoretical predictions, primarily due to the kinetic conditions of the reaction. According to the Tafel equation[69] (Eq. 2):

$$\eta = b\log i + a \quad (2)$$

where η denotes the overpotential, b is the Tafel constant, i is the current density, and a is the overpotential at unit current density. The overpotential η is primarily influenced by a[70], and the intrinsic properties of zinc metal lead to a higher overpotential at unit current density. Specifically, the high Tafel slope (approximately 0.12 V) and the high Tafel intercept (1.24 V) for HER result in a substantial overpotential, which limits HER, particularly at higher rates[50]. Considering both kinetic and thermodynamic factors, zinc ions preferentially gain electrons and deposit on the anode surface, thereby inhibiting HER during the charging process. However, HER is also affected by other factors, such as temperature[71] and the surface morphology of the zinc anode[72]. Consequently, in some cases, HER may become problematic and compromise the safety of ZIBs[73].

2.3 Corrosion phenomena

Electrochemical corrosion in ZIBs leads to electrode passivation, causing the continuous consumption of active materials such as zinc metal and electrolyte during cycling[74](Figs. 3a and 3b). For instance, in mildly acidic electrolytes, "dead zinc", formed by the detachment of dendrites at the anode, loses its electrochemical activity. In addition, the HER increases the concentration of OH^- near the anode. Due to electrostatic attraction, the net positive charges continuously draw OH^- and SO_4^{2-} to react[75]. These reactions result in the formation of insoluble by-products, such as $ZnSO_4[Zn(OH)_2]_3{\cdot}xH_2O$ (ZSH) (Fig. 3b)[60,76,77], which precipitate on the anode surface. This process negatively impacts battery performance by reducing Coulombic efficiency and increasing impedance. The formation of ZSH in mildly acidic electrolytes is similar to that of ZnO in alkaline electrolytes[47]. A similar phenomenon occurs at the cathode, where the by-product

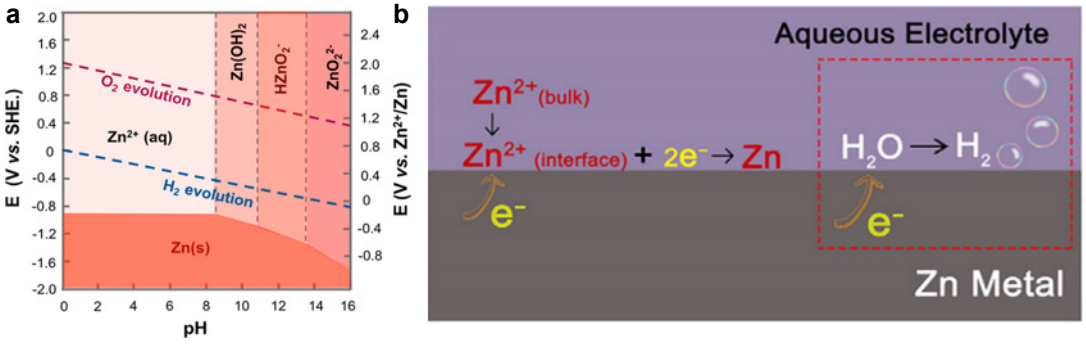

Figure 2 (a) Pourbaix diagram for 10^{-6} mol L^{-1} Zn^{2+}. Reproduced under the CC BY 4.0 license from Ref. [64] ©2016, The Authors. (b) Schematic of hydrogen evolution. Reproduced with permission from Ref. [62] ©2018, Elsevier Ltd.

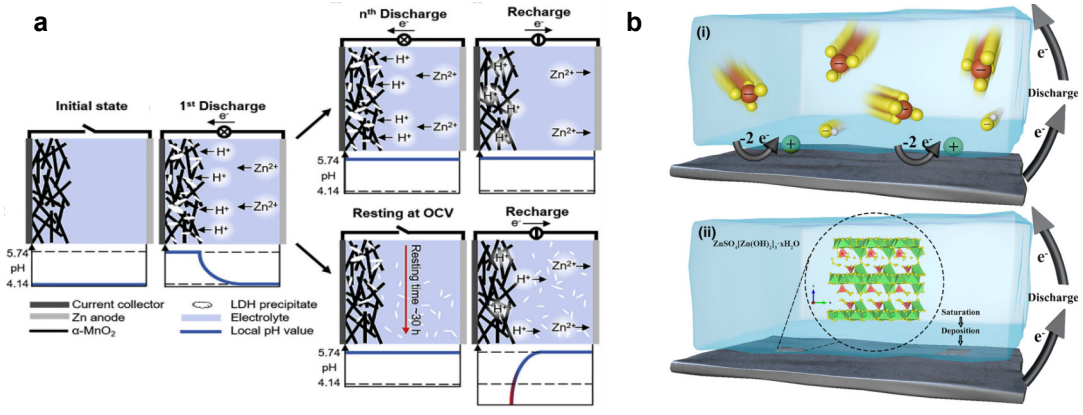

Figure 3 (a) Schematic of $Zn_4(OH)_6SO_4{\cdot}xH_2O$ (LDH) formation at the cathode. Reproduced with permission from Ref. [78] ©2019, American Chemical Society. (b) Schematic of $ZnSO_4[Zn(OH)_2]_3{\cdot}xH_2O$ (ZSH) formation on the anode surface. Reproduced with permission from Ref. [60] © 2020, Zhengzhou University.

$Zn_4(OH)_6SO_4{\cdot}xH_2O$ (LDH) forms, as shown in Fig. 3a[78].

The formation and dissolution of LDH cause fluctuations in the electrolyte's pH, which in turn accelerates the anode's corrosion. Meanwhile, Zn^{2+} ions combine with OH^- and SO_4^{2-} in the electrolyte to form ZSH and other by-products[37,79]. Although this buffering mechanism supports the reversible operation of ZIBs, it also introduces significant drawbacks[78,80]. For example, LDH can delaminate from the cathode surface, compromising the stability of the cathode materials. After extended cycling, LDH tends to detach from the cathode, leading to a rapid decline in electrochemical performance[58]. Whether passivation occurs at the cathode or anode, it results in the continuous consumption of active materials, reducing Coulombic efficiency, increasing impedance, impairing ion transport, and ultimately degrading the electrochemical performance of ZIBs.

2.4 Interaction of dendrites, HER and corrosion

In practical electrochemical processes, the challenges in aqueous ZIBs—dendrite formation, HER, and corrosion—do not occur independently but interact and exacerbate one another. For example, dendrite formation increases the surface area of the electrode, and the rough surface morphology is a key kinetic factor in promoting HER[67]. The larger surface area also provides more active sites for HER to occur. Moreover, intense HER depletes H^+, leading to a rapid increase in OH^- concentration in the local environment, which in turn accelerates passivation reactions. The insoluble by-products from passivation not only aggravate the "tip effect", increasing electrode polarization and accelerating dendrite growth[52], but also provide additional active sites for HER. As a result, these issues reinforce each other, forming a vicious cycle that eventually compromises the stability and performance of the entire battery system.

Therefore, when addressing these problems, the overall impact of the chosen solution on the entire battery system must be considered. It is essential to evaluate whether a proposed modification mitigates multiple issues or inadvertently exacerbates others.

3 Strategies summary

To address the aforementioned issues, researchers have explored various strategies. There are two critical interfaces in the zinc metal anode: the interface between the zinc metal and the current collector, and the interface between the zinc metal and the electrolyte. These interfaces directly impact the anode's performance. Zinc deposition involves two key processes: nucleation and growth. Achieving a uniform distribution of ions and electrons at these interfaces is essential for consistent deposition. Uneven nucleation on the anode surface exacerbates imbalances in electron and ion concentrations, worsening the previously mentioned challenges[27]. Current solutions primarily focus on ensuring uniform ion and electron distribution and can be categorized into four approaches: 1. structural design; 2. surface modification; 3. electrolyte optimization; 4. alloying anode.

3.1 Structural design

The primary goal of structural design is to enhance the contact area between the current collector and the electrode surface, reduce local charge density, decrease nucleation overpotential, and achieve dendrite-free deposition by minimizing uneven electrolyte concentration and electric field distribution. The rate of zinc deposition is heavily influenced by polarization during electroplating, as even small overpotentials can significantly disrupt the electric field. To mitigate polarization, substantial research has focused on designing substrates with increased specific surface area and local current density,

thereby reducing polarization during zinc deposition.

The 3D porous dual-channel structure of zinc electrodes can effectively balance ion and electron conduction, significantly suppressing dendrite growth and side reactions (Fig. 4a)[81]. Consequently, batteries equipped with the as-prepared DCP-Zn anodes exhibit prolonged cycle life (up to 1400 h at 0.1 mAh cm^{-2}) and high energy density (333.8 Wh kg^{-1}). Carbon-based materials are widely used as current collectors due to their high conductivity, enabling rapid electron transfer across the electrodes and maintaining a uniform electric field. For example, the strong interaction between Zn and single vacancy defects limits Zn diffusion on the anode surface, causing Zn nuclei to accumulate at defective carbon sites (Fig. 4b)[82]. Benefiting from the carbon fiber substrate, the carbon-decorated electrode achieves dendrite-free Zn deposition, with Coulombic efficiency exceeding 97% over 5000 cycles. Lu et al.[83] reported a carbon nanotube zinc anode (CNT/Zn), which features carbon nanotubes attached to flexible carbon cloth. During zinc deposition, the zinc metal grows around the carbon nanotubes without forming significant dendrites, as confirmed by scanning electron microscopy (SEM) (Fig. 4c). Carbon nanotubes also reduce the nucleation overpotential due to their superior electrical conductivity. The authors performed theoretical calculations on the electric field distribution after zinc nucleation, confirming the uniformity of the electric field in the CNT/Zn anode. In addition, Xue et al.[84] mixed reduced graphene oxide (rGO) with CNTs to create a Zn metal composite anode with 3D scaffolds, which homogenizes ion flow and mitigates

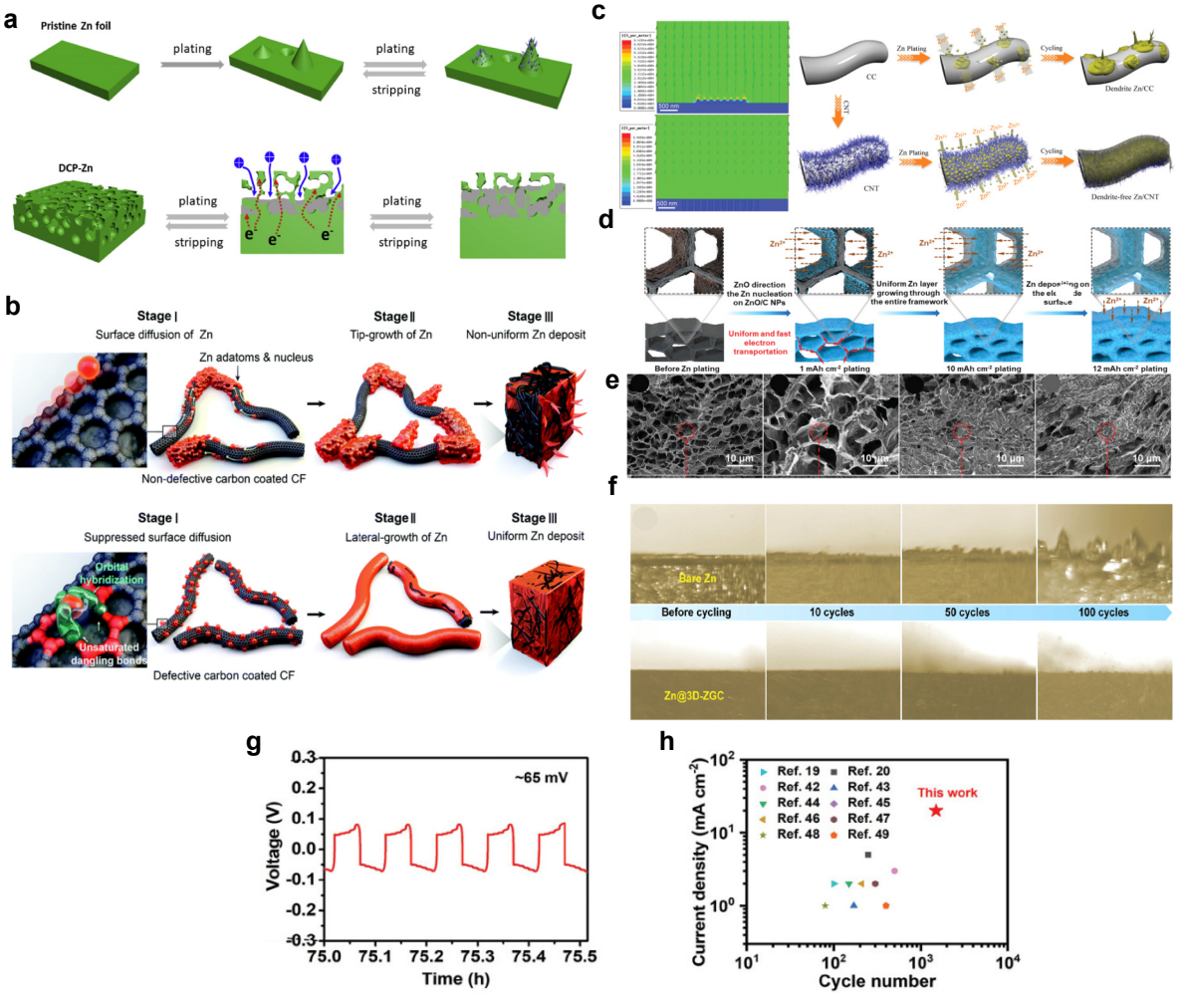

Figure 4 (a) Illustrative comparison of original Zn foil and DCP-Zn. Reproduced with permission from Ref. [81] ©2020, Elsevier B.V. (b) Schematic of Zn plating on carbon fiber, showing homogeneous Zn nucleation and lateral deposition. Reproduced with permission from Ref. [82] ©2020, Elsevier B.V. (c) Schematic illustrations of Zn deposition on CC and CNT Zn anodes. Reproduced with permission Ref. [83] ©2019, WILEY-VCH Verlag GmbH & Co. KGaA, Weinheim. (d) Schematic illustration of the 3D-ZGC scaffold. (e) Cross-sectional SEM images of the 3D-ZGC scaffold upon Zn metal deposition with varying plated Zn metal amounts. (f) In situ optical microscopy visualization of Zn plating behavior on bare Zn foil and 3D-ZGC anode. (g) Detailed voltage profiles of the 3D-ZGC anode. (h) Comparison of symmetrical cells with the Zn@3D-ZGC composite anode and previously reported anodes. Reproduced with permission from Ref. [84] ©2022, Wiley-VCH GmbH.

anode volume changes (Fig. 4d). The as-prepared 3D-ZGC electrode showed negligible morphological changes after 1 mAh cm^{-2} of plating (Fig. 4e). Even at an ultrahigh current density of 20 mA cm^{-2}, no significant protuberance was observed on the 3D-ZGC anode surface under optical microscopy (Fig. 4f). Long-term cycling further confirmed the smaller overpotential of the 3D-ZGC anode, demonstrating its ability to promote uniform Zn deposition (Fig. 4g). Notably, a flexible polyimide-tape-supported Zn/hydrophilic carbon nanotube with oxygen-containing functional groups was applied to address the shuttle effect of I_3^-, benefiting from the carbon nanotube structure and the abundant oxygen-containing functional groups[85]. Compared to previously reported 3D Zn composite anodes, the 3D-ZGC anode exhibits unparalleled cycling stability (Fig. 4h). Guo et al.[86] used highly conductive carbon fiber-graphite felt (GF) as a current collector, electrodepositing zinc under constant voltage to manufacture a Zn@GF anode. The plating/stripping of Zn on GF demonstrated exceptional cycling stability with minimal potential fluctuation. When assembled into a full coin cell coupled with an HQ-PB cathode, the battery with the Zn@GF anode showed impressive rate capability. The GF provided a larger electroactive surface area, allowing for faster electron transport and increased electrolyte permeability.

Xu et al.[87] reported a 3D porous copper skeleton zinc metal anode designed to ensure the homogeneous deposition and stripping of Zn. This anode was prepared by electrodepositing Zn onto a chemically etched porous copper skeleton. The porous structure allows the aqueous electrolyte to penetrate evenly through the copper framework, increasing the diffusion rate of Zn^{2+} ions and reducing the polarization of Zn^{2+} reduction, which helps inhibit dendrite growth, HER, and corrosion. In addition, the high conductivity of copper ensures rapid electron transfer across the entire anode framework. As a result, the 3D porous copper anode achieves uniform ion concentration and electric field distribution, essential for preventing zinc dendrites.

To achieve high current density/capacity and stable cycling performance, Guan et al.[88] designed a gradient Zn anode with gradient conductivity and hydrophilicity. The anode features a double-gradient structure, with a top hydrophobic and insulating layer of PVDF and a bottom hydrophilic and conductive layer of Sn. This structure effectively prevents corrosion and inhibits HER due to the high redox potential of the Sn layer. The imprinted gradient Zn anode exhibited stable cycling for 1200 h at a low current density of 1 mA cm^{-2} and for 200 h at a high current density/capacity of 10 mA cm^{-2}/10 mAh cm^{-2}.

However, the complex structure of such anodes requires intricate fabrication processes and is prone to damage during cycling. In addition, the high cost of Zn-based substrates poses a challenge to further development in structural design. While anodes with larger surface areas can mitigate dendrite growth and corrosion, they also present more active sites for HER. Future advancements in structural design should focus on enhancing the toughness of 3D structures to accommodate volume changes during cycling, simplifying manufacturing processes, and reducing costs.

3.2 Surface modification

The goal of surface modification is to inhibit dendrite growth by creating a protective layer on the surface of the Zn metal anode that conducts ions or electrons and ensures their uniform distribution[89–93]. This artificial layer acts as an ion filter, reducing shape changes, inhibiting dendrite growth, and preventing direct contact between the anode and the electrolyte, which can effectively minimize the occurrence of HER and corrosion. During the charging process, Zn deposition involves at least four successive steps: Zn^{2+} diffusion, Zn^{2+} reduction, Zn nucleation, and Zn crystal growth[94]. Among these steps, Zn nucleation and crystal growth must overcome energy barriers, which are closely related to the electrochemical environment. A lower energy barrier promotes uniform Zn deposition, and a faster Zn^{2+} diffusion rate helps reduce electrolyte concentration polarization.

The surface coating layer must possess high electronic or ionic conductivity, limit surface 2D diffusion, remain stable in water, exhibit good wettability with the electrolyte, show excellent affinity with the Zn anode, and have sufficient mechanical strength to accommodate volume changes.

Zincophilic sites are crucial for achieving uniform Zn deposition. As shown in Fig. 5a, widely distributed zincophilic sites promote the connection between adjacent nuclei, leading to homogeneous Zn deposition[95]. Inspired by this mechanism, our group developed a multicomponent copper–zinc alloy layer with superior Zn affinity and high toughness on Zn foil to fabricate an ultra-stable Zn metal anode (Cu–Zn@Zn). The Cu–Zn alloy layer offers several advantages. First, due to the high binding energy between the Cu–Zn alloy and deposited Zn atoms, the Cu–Zn@Zn electrode significantly increases nucleation sites by limiting the diffusion of Zn atoms on the surface, thereby reducing Zn atom aggregation and enhancing the uniformity of Zn deposition (Fig. 5b). Second, the copper–zinc alloy acts as a buffer layer, effectively mitigating lattice distortion during cycling and reducing the direct contact between the electrode and electrolyte, thus inhibiting HER and corrosion. As a result, the symmetric

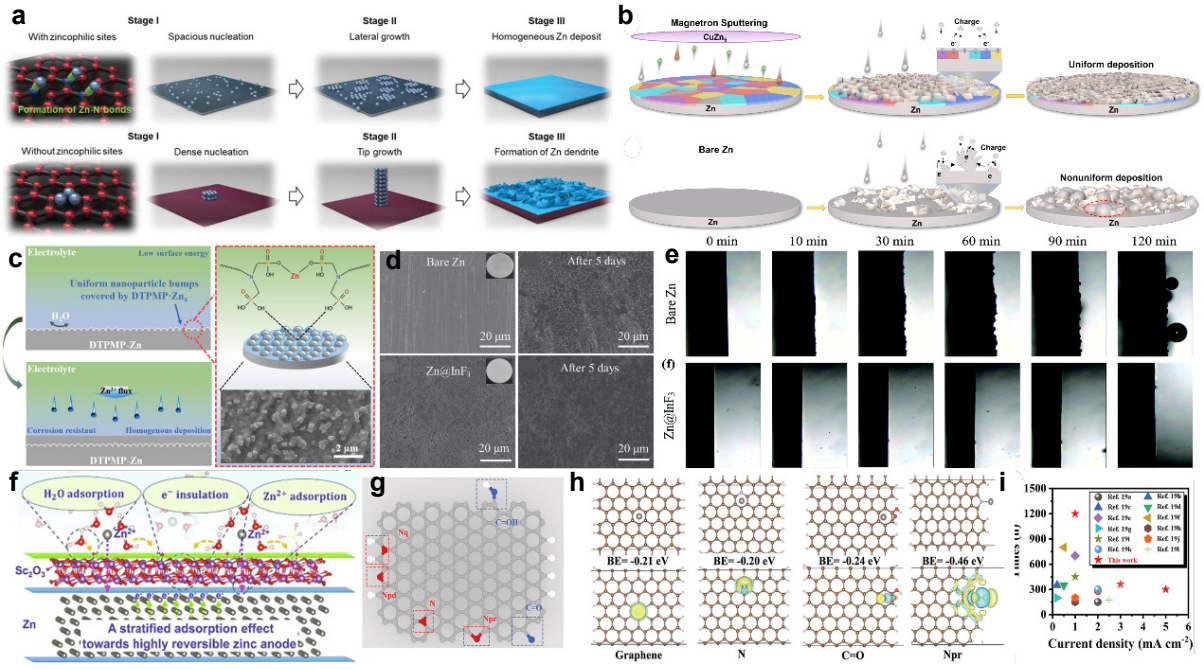

Figure 5 (a) Schematic of Zn deposition on surfaces with and without zincophilic sites. Reproduced with permission from Ref. [95] ©2021, Wiley-VCH GmbH. (b) Schematic illustration of Zn deposition on Cu–Zn@Zn and bare Zn electrodes. Reproduced with permission from Ref. [96] ©2022, Wiley-VCH GmbH (c) Schematic illustration of the initial stage and plating on the DTPMP-Zn anode. Reproduced with permission from Ref. [97] ©2022, American Chemical Society. (d) Bare Zn and Zn@InF_3 before and after immersion in 2 mol/L $ZnSO_4$. (e) *In situ* optical microscopy observation of zinc deposition morphology on Zn and Zn@InF_3 electrodes. Reproduced with permission from Ref. [98] ©2022, Tsinghua University Press. (f) Schematic diagram of the reaction process on the Sc_2O_3-coated Zn anode. Reproduced with permission from Ref. [99] ©2020, Science Press and Dalian Institute of Chemical Physics, Chinese Academy of Sciences. (g) Configuration of N-doped graphene oxide (NGO). (h) Schematic diagram and DFT calculation of the binding energy of a Zn atom on graphene. (i) Comparison of cycle performance and current density of NGO@Zn anodes with other reported anodes. Reproduced with permission from Ref. [100] ©2021, Wiley-VCH GmbH.

battery with the Cu–Zn@Zn electrode exhibits an ultra-long cycle life of 5496 h at 1 mA cm^{-2} for 1 mAh cm^{-2}, with a low overpotential of 30 mV. This performance is significantly better than previously reported AZIB results under similar conditions. In addition, the Cu–Zn@Zn//V_2O_5 pouch cell demonstrates excellent cycling stability, retaining 88% of its capacity after 600 cycles[96]. Other metals similarly provide zincophilic sites. For instance, Li et al.[101] prepared a tin-modified zinc metal anode using magnetron sputtering, a physical vapor deposition technique known for its simplicity, ease of control, large coating area, and strong adhesion. In this study, a tin layer was first deposited onto a carbon felt substrate, followed by electrochemical deposition of zinc. Theoretical calculations indicate that the adsorption energy between tin and zinc is 2.5 times higher than that between zinc atoms. Charge–density analysis further revealed that the strong electronic interactions and polarization significantly enhance the bond between Sn and Zn. This strong adsorption prevents the two-dimensional diffusion of zinc ions on the anode surface, which is a primary cause of dendrite formation. In addition, the strong binding force helps prevent the deposited zinc from detaching from the current collector, thereby reducing the formation of "dead zinc." Sputtering tin also significantly inhibits hydrogen evolution reactions. These combined advantages ensure the excellent electrochemical performance of the tin-modified zinc metal anode. The affinity between the Zn substrate and surface protective layer materials plays a crucial role in lowering the energy barrier for Zn nucleation and crystal growth. A low energy barrier reduces the polarization of Zn deposition, which is essential for achieving a homogeneous morphology in newly deposited Zn. Compared to inorganic modification layers, which are prone to cracking and damage due to low toughness and weak binding strength with the Zn substrate during cycling, metal modification materials exhibit higher toughness, allowing them to adapt to the volume changes of the Zn anode[102,103]. Moreover, the strong affinity between the modification layer and the Zn substrate promotes uniform Zn deposition. For instance, Chen et al.[92] reported a silver particle-coated zinc plate prepared via a simple replacement reaction. Unlike the faceted TiO_2 coating mechanism, the newly formed $AgZn_3$ alloy has strong zinc affinity, which effectively reduces the energy barrier for nucleation and enables uniform zinc deposition. The symmetrical battery with the Zn@Ag anode demonstrated stable cycling for 1700 h

at 0.25 mA cm^{-2} and 0.25 mAh cm^{-2}. Alloy modification materials also support uniform Zn deposition. Cu–Zn alloys, frequently used due to their low cost and stable performance, are ideal for electrodes. For example, a Zn_xCu_y alloy shell was constructed on a self-supported three-dimensional nanoporous Zn anode, guiding uniform Zn deposition and facilitating Zn stripping[104]. However, spontaneous alloying reactions between deposited Zn atoms and metallic Cu can create new alloys with different crystal structures than Zn and Cu, leading to severe lattice distortion, increased internal stress in the anode, and compromised interface stability between the modification layer and Zn substrate[105–107].

Organic molecular surface modification layers with acid groups can also create numerous zincophilic sites. For instance, the hydrophobic Zn_x-diethylenetriaminepenta (methylene-phosphonic acid) layer (DTPMP) not only naturally resists water, reducing direct contact between the anode and electrolyte, but also promotes ion diffusion (Fig. 5c)[97]. Inorganic compounds can also serve as protective layers. Qian et al.[98] coated a layer of InF_3 on a Zn metal anode, which remained relatively flat after immersion in 2 mol/L $ZnSO_4$ for 10 days (Fig. 5d). Furthermore, *in situ* optical microscopy revealed dense Zn plating with no bubble formation on the Zn@InF_3 anode (Fig. 5e). In addition, a hydrophilic Sc_2O_3 layer can capture and immobilize H_2O from $[Zn(H_2O)_6]^{2+}$, reducing the amount of active water molecules and facilitating the desolvation of Zn^{2+} (Fig. 5f)[99].

In addition, to developing zincophilic-rich surface modification layers, some researchers have focused on constructing a coherent or semi-coherent host/zinc interface based on crystal lattice structures[108]. Zheng et al.[109] discovered a method for epitaxially depositing metals. In previous studies, it was observed that zinc is a close-packed hexagonal metal. During electrochemical deposition, Zn ions tend to deposit in a way that exposes the (0002) close-packed plane, minimizing thermodynamic free energy. The authors used a liquid flow shearing method to successfully prepare graphene sheets with a specific (0001) crystal plane orientation. Due to the low lattice mismatch between these two crystal planes, zinc metal combines with the graphene substrate on this plane and grows epitaxially along the normal direction, maintaining a locked orientation relationship with the graphene substrate. After deposition, the zinc metal grows in flake-like structures on the substrate. Similarly, Wang et al.[108], starting from crystal orientation, constructed a specific faceted titanium dioxide (TiO_2) with relatively low zinc affinity as a protective layer for the zinc anode. They coated different facets of TiO_2 on Zn foil and found that TiO_2 with a highly exposed (001) facet exhibited the best electrochemical performance. The anode prepared with this coating demonstrated a long lifespan of 460 h at 1 mA cm^{-2} for 1 mAh cm^{-2} with low voltage hysteresis. Due to its low affinity for Zn, the faceted TiO_2-coated Zn anode surface can accumulate Zn^{2+} ions, leading to uniform nucleation and deposition. In addition, annealing the Zn metal anode can repair lattice defects and relieve residual stress, promoting highly epitaxial electrodeposition and enhancing reversible electrochemical behavior[110]. Since defects and residual stresses are likely to promote dendrite formation, Wang et al.[100] suggested that the Zn (002) facets may not be optimal for epitaxial growth. Instead, a randomly oriented substrate can also facilitate epitaxial zinc growth, even though the deposited zinc is randomly oriented. Nitrogen-containing functional groups in N-doped graphene oxide (NGO) primarily consist of pyrrole groups (Fig. 5g). Theoretical calculations indicate that these pyrrole groups interact strongly with Zn atoms due to the favorable semi-coherent host/zinc interface (Fig. 5h), which reduces polarization voltages. As a result, symmetric batteries with NGO@Zn anodes exhibit significantly improved cycling life and performance at high current densities compared to previously reported modified Zn anodes (Fig. 5i).

Metal-organic framework (MOF) materials are a type of coordination polymer that have developed rapidly over the past decade. These materials feature a three-dimensional porous structure, with metal ions and organic ligands acting as connection points to form an extended 3D network. Zhou et al.[90] constructed a MOF material as a front surface layer to maintain a super-saturated electrolyte layer. Due to the porous structure of the MOF layer, a significant portion of water is rejected through partial desolvation, resulting in a super-saturated electrolyte within the MOF channels. Benefiting from this unique super-saturated front surface, symmetric Zn cells exhibited exceptional stability, lasting up to 3000 h at 0.5 mA cm^{-2} and 0.5 mAh cm^{-2}.

In summary, surface modification offers several advantages, including promoting uniform Zn deposition, effectively suppressing HER and corrosion, being cost-effective, and environmentally friendly. However, the ideal "thickness" of the modification layer remains a topic of debate. As thickness increases, the charge transfer impedance also rises, while the effect of lowering the nucleation energy barrier diminishes, reducing the effectiveness of dendrite inhibition[111]. Conversely, if the layer is too thin, it may exacerbate surface unevenness on the anode. Thus, future research on surface modification should focus on determining the optimal thickness for balancing these effects.

3.3 Electrolyte optimization

Various types of electrolytes are used in ZIBs, including aqueous, organic, gel, ionic liquid, and solid electrolytes[112]. Aqueous electrolytes are the most widely used due to their high ionic conductivity, low cost, and environmentally friendly nature. In addition, they have a high Zn^{2+} ion concentration and diffusion rate, which alleviates concentration polarization and promotes uniform Zn deposition[31,113]. Current electrolyte modification strategies for inhibiting dendrite growth, HER, and corrosion in aqueous systems mainly focus on three aspects:

1. Species of zinc salt. Different zinc salts are used in electrolytes, such as $ZnCl_2$, $Zn(NO_3)_2$, $ZnSO_4$ and $Zn(CF_3SO_3)_2$[114–116]. $ZnSO_4$ is cost-effective, while $Zn(CF_3SO_3)_2$ offers higher solubility and a broader electrochemical window[116]. The large $CF_3SO_3^-$ anion disrupts the tightly solvated sheath around zinc ions, promoting better electrochemical performance. In contrast, $ZnCl_2$ and $Zn(NO_3)_2$ electrolytes exhibit irreversible electrochemical behavior due to the instability of Cl^- and NO_3^-[49,117].

2. Zinc salt concentration. In mildly acidic electrolytes, zinc ions form solvation sheaths by coordinating with water molecules. During electrochemical deposition, zinc ions must first undergo a desolvation process, which requires additional energy and slows the reaction kinetics. Increasing the zinc salt concentration reduces the amount of coordinated water, thereby lowering desolvation energy and accelerating electrode reactions[118]. For example, high-concentration $Zn(CF_3SO_3)_2$ electrolytes demonstrate superior stability by weakening the solvation effect (Fig. 6a)[119]. In addition, a sufficiently high concentration of bis(trifluoromethane)sulfonamide ($TFSI^-$) anions can lead to the formation of anhydrous solvation sheaths, where six $TFSI^-$ anions coordinate with Zn^{2+} (Fig. 6b), resulting in exceptional cycling stability (Fig. 6c)[120]. Furthermore, reducing the coordination number of Zn^{2+} with H_2O decreases the likelihood of water reduction to hydrogen during Zn deposition, mitigating HER and corrosion[121].

3. Organic additives and metal ion additives. Theses are two main types of electrolyte additives that currently used to enhance the performance of ZIBs. Organic additives can inhibit dendrite formation on the anode. From the perspective of adjusting crystal orientation, sodium dodecyl sulfate effectively induces oriented Zn deposition along the (002) plane, resulting in a dense and uniform electrochemical morphology[122]. The additive CH_3COONH_4, which preferentially adsorbs on the zinc anode, reduces the activity of water at the anode–electrolyte interface. During cycling, the resulting $Zn_5(CO_3)_2(OH)_6$ solid electrolyte interphase functions as a protective layer that conducts Zn^{2+} and ensures uniform Zn deposition (Fig. 6d)[123]. A symmetric battery using CH_3COONH_4-based electrolyte can operate stably at an ultrahigh current density of 40 mA cm^{-2} with a cumulative capacity of 6880 mAh cm^{-2}. Deep eutectic solvents (DES) are non-flammable, eco-friendly, and compatible with metal salts. Mai et al.[124] developed a $ZnCl_2$/ethylene glycol (EG) hybrid eutectic electrolyte. The H-bond donor EG replaces the water molecules in $[Zn(H_2O)_6]^{2+}$ and forms $[ZnCl(EG)]^+/[ZnCl(EG)_2]^+$ cations, guiding Zn^{2+} flux (Fig. 6e). As a result, a symmetric battery using $ZnCl_2$/EG electrolyte achieved 2000 h of stable cycling (Fig. 6f). From the perspective of reducing the nucleation energy barrier, Wang et al.[125] reported a polyacrylamide (PAM) electrolyte additive. Changes in Raman peak intensity indicated that the PAM chain attaches to the anode copper net (Fig. 6g). During cycling, the PAM chain acts as a buffer layer for zinc-ion deposition, effectively inhibiting dendrite formation. Similarly, a polyacrylamide/reduced graphene oxide molecular nanobrush coating on the Zn anode consolidates uniform Zn deposition by utilizing the zincophilic functional groups of the branched polyacrylamide chain and the high conductivity of reduced graphene[126]. To lower the desolvation energy barrier, Tao et al.[127] designed a water-in-DES electrolyte based on a $ZnCl_2$-acetamide DES. This unique Zn^{2+} solvation structure enables a lower dissociation energy barrier and nucleation overpotential, leading to uniform Zn deposition (Figs. 6h and 6i). In addition, polarized organic molecules can provide an electrostatic shielding effect. Xu et al.[128] used diethyl ether (Et_2O) to mitigate dendrite growth by adsorbing Et_2O onto newly deposited Zn protuberances, forming an electric field that restrains dendrite growth.

Metal ion additives can also significantly impact zinc-ion battery performance. When the added metal ions have a higher redox potential than Zn^{2+}, they are deposited preferentially, acting as a substrate for zinc deposition. If their redox potential is lower, the metal ions do not participate in the electrochemical reaction but instead create an electrostatic shield. Specifically, introduced metal cations accumulate around incipient Zn nuclei due to the "tip effect", forming an electrostatic shield with a strong positive electric field that prevents the continued accumulation of Zn^{2+}[129,130]. Niu et al.[131] added Na_2SO_4 to a $ZnSO_4$ electrolyte, which not only reduced dendrite formation at the zinc anode but also slowed the dissolution of sodium vanadate hydrate cathode materials during cycling. The capacity of Na_2SO_4 additive-based ZIBs remained stable at 221 mAh g^{-1} after 100 cycles. The electrochemical performance of batteries at low temperatures is a critical indicator of their practical application potential. Introducing inorganic salts into aqueous electrolytes is a simple and cost-effective

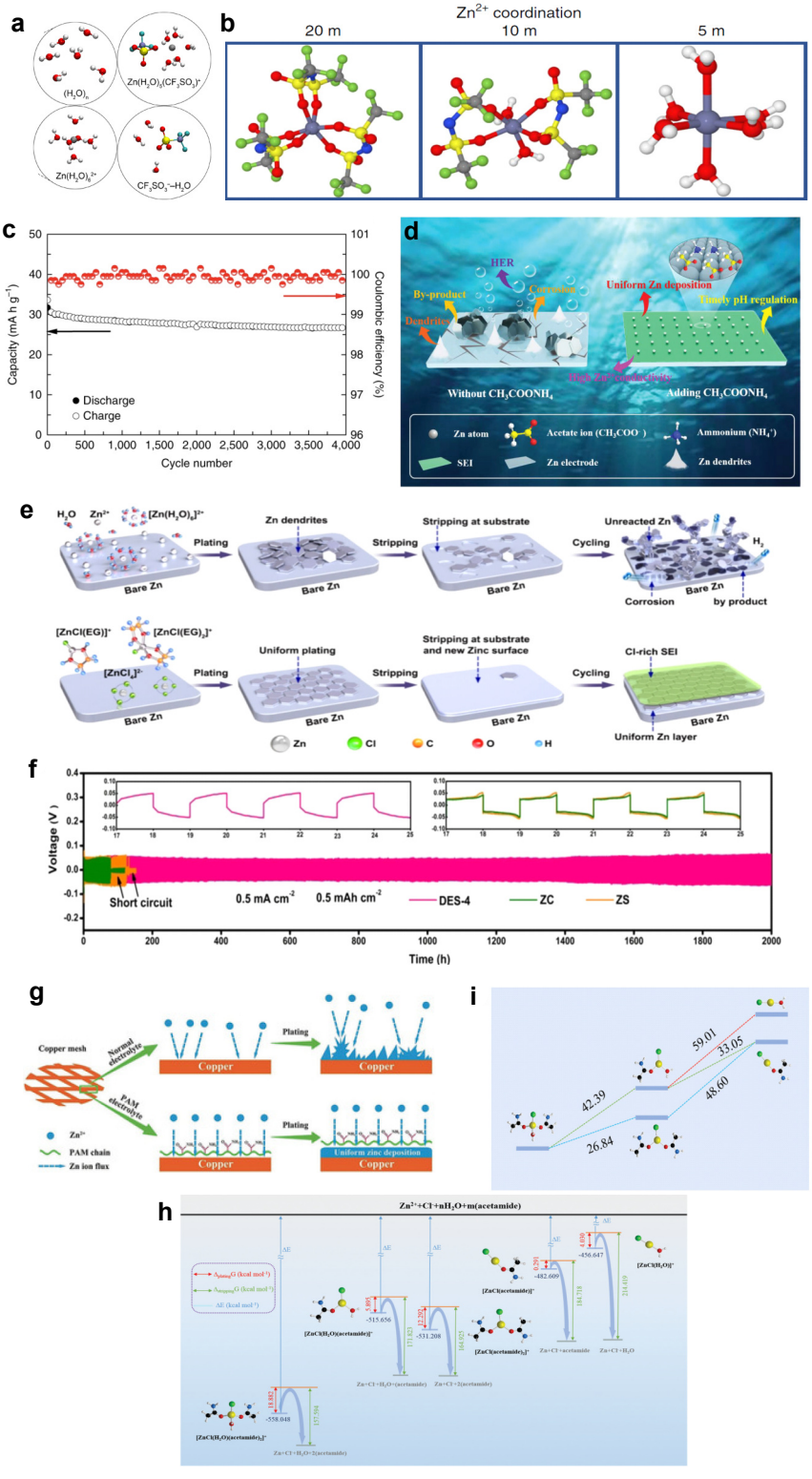

Figure 6 (a) Molecular dynamics simulations of Zn^{2+} solvation structures. Reproduced with permission from Ref. [119] ©2021, American Chemical Society. (b) Zn^{2+} solvation structures in TFSI-based electrolytes at different concentrations. (c) Cycling stability and Coulombic efficiency of Zn/$LiMn_2O_4$ full cells in HCZE at 4 C. Reproduced with permission from Ref. [120] ©2018, The Author(s). (d) Schematic illustration of interfacial evolution in CH_3COONH_4 additive-modified vs. unmodified electrolytes. Reproduced under the CC BY 4.0 license from Ref. [123] ©2022, The Authors. (e) Zn plating/stripping scheme in aqueous electrolyte and $ZnCl_2$/EG eutectic electrolyte. (f) Galvanostatic Zn plating/stripping with DES-4 and ZS electrolytes. Reproduced with permission from Ref. [124] ©2022, Wiley-VCH GmbH. (g) Schematic diagram of Zn plating on copper mesh 3D zinc anode with PAM electrolyte additive. Reproduced with permission from Ref. [125] ©2019, Wiley-VCH Verlag GmbH & Co. KGaA, Weinheim. (h) Schematic energy demonstration, including dissociation, plating, and stripping activation in the water-in-DES electrolyte. (i) Illustration of Zn^{2+} desolvation/solvation in the water-in-DES electrolyte. Reproduced with permission from Ref. [127] ©2021, Wiley-VCH GmbH.

antifreeze strategy. The interaction of ions from salt solutes with water disrupts the hydrogen-bond network between water molecules, inhibiting ice crystal nucleation and lowering the freezing point of water. Mai et al.[132] revealed the correlation between tetrahedral entropy and freezing point, constructing a high-entropy $Zn(ClO_4)_2$ electrolyte that demonstrated long cycle stability at −80 °C.

As a critical component of aqueous electrolytes, the separator plays a vital role in battery performance. Sun et al.[133] developed a Janus separator by directly growing a vertical graphene carpet on one side of a commercial glass fiber separator. The large surface area and porous structure of the Janus separator provide homogeneous electric field distribution and low local current density. To enhance zincophilicity, oxygen and nitrogen heteroatoms were co-doped onto bare graphene through a simple air plasma treatment, ensuring uniform Zn ionic flux. This strategy resulted in remarkable rate and cycle performance for Zn-ion hybrid capacitors and excellent capacity for ZIBs.

In addition, to aqueous electrolytes, many studies focus on organic, gel, ionic liquid, and solid electrolytes[134,135]. In ZIBs, the use of solid-state electrolytes is also an effective strategy to mitigate dendrite formation and side reactions such as HER and passivation. Currently, solid-state ZIBs primarily use hydrogel electrolytes[17,136], which are quasi-solid-state electrolytes. However, hydrogel electrolytes are prone to water loss and exhibit poor mechanical properties, greatly limiting their application in solid-state ZIBs. Zhi et al.[137] prepared an ionic-liquid-based Zn salt electrolyte, achieving highly reversible, dendrite-free, and non-hydrogen-evolving Zn deposition and dissolution. Furthermore, the authors constructed a 28.6 μm-thick solid polymer electrolyte composed of a poly(vinylidene fluoride-hexafluoropropylene) film filled with poly(ethylene oxide) and ionic-liquid-based Zn salt. This electrolyte demonstrated high ionic conductivity (16.9 mS/cm), excellent flexibility, and strong mechanical properties. Solid-state and hydrogel electrolytes are highly efficient at suppressing dendrite growth, inhibiting HER, and preventing corrosion, making them promising candidates for high-performance ZIBs.

In general, improving aqueous electrolytes is crucial for regulating Zn deposition. However, the high cost of additives limits their broader commercialization. A deeper understanding of the effects of electrolyte additives on electrochemical processes, as well as achieving stability at the electrolyte–electrode interface, are key to developing effective electrolyte modification strategies. Reducing costs is essential for practical applications.

3.4 Alloying anode

The alloying design of the anode has recently been extensively studied. Compared with traditional zinc metal anodes, zinc alloy anodes offer unique properties. In these alloys, zinc serves as the active material, while other metals provide functional properties. For instance, Cu–Zn alloys have been used as anode materials for high-performance ZIBs[138–140]. Cu/Zn composites, Zn/porous Cu hosts, and brass help mitigate chemical corrosion and dendrite formation, significantly improving the electrochemical performance of ZIBs.

Jiang et al.[141] reported a layered zinc–aluminum (Zn–Al) alloy anode. According to the Zn–Al alloy phase diagram, the eutectic point occurs at $Zn_{88}Al_{12}$ (at%). As shown in Fig. 7a, the alloy formed at the eutectic point resembles pearlite, exhibiting a layered structure. Different condensation rates control the thickness of the zinc and aluminum layers. Due to aluminum's chemically active nature, it forms a dense oxide layer. During the deposition process, this aluminum oxide layer is non-conductive, meaning that zinc can only be deposited between the aluminum layers, effectively inhibiting dendrite growth. Batteries with $Zn_{88}Al_{12}$alloy anodes and K_xMnO_2 cathodes deliver high energy density and retain 100% capacity after 200 h.

Yang et al.[142] prepared a zinc–manganese (Zn–Mn) alloy anode. As shown in Fig. 7b, zinc is plated into the 3D pores of manganese metal, forming a Zn_3Mn alloy, which provides a fast diffusion path for zinc ions, enabling thorough electrolyte permeation and a more uniform ion concentration. In addition, the cauliflower-like 3D structure mechanically inhibits dendrite formation. The Zn–Mn alloy anodes demonstrated stability over thousands of cycles, even under harsh electrochemical conditions.

The aforementioned alloying designs focus on modifying the anode structure, either by leveraging the charge shielding effect of the alloy or constructing a 3D current collector to suppress dendrites. Some researchers have also explored surface alloying. As illustrated in Figs. 7c–7e, Chen et al.[105] coated the zinc metal anode surface with a layer of liquid gallium–indium (Ga–In) alloy. This alloy possesses extremely high electronic and ionic conductivity. During the zinc deposition process, Zn gradually diffuses from the Ga–In alloy surface to the substrate due to the Zn concentration gradient. According to the thermodynamic phase diagram, once the zinc concentration reaches a threshold, zinc metal precipitates beneath the Ga–In alloy, effectively inhibiting dendrite growth. In addition, the presence of this buffer layer prevents direct contact between the zinc metal and the electrolyte, reducing the occurrence of hydrogen evolution and passivation reactions. A

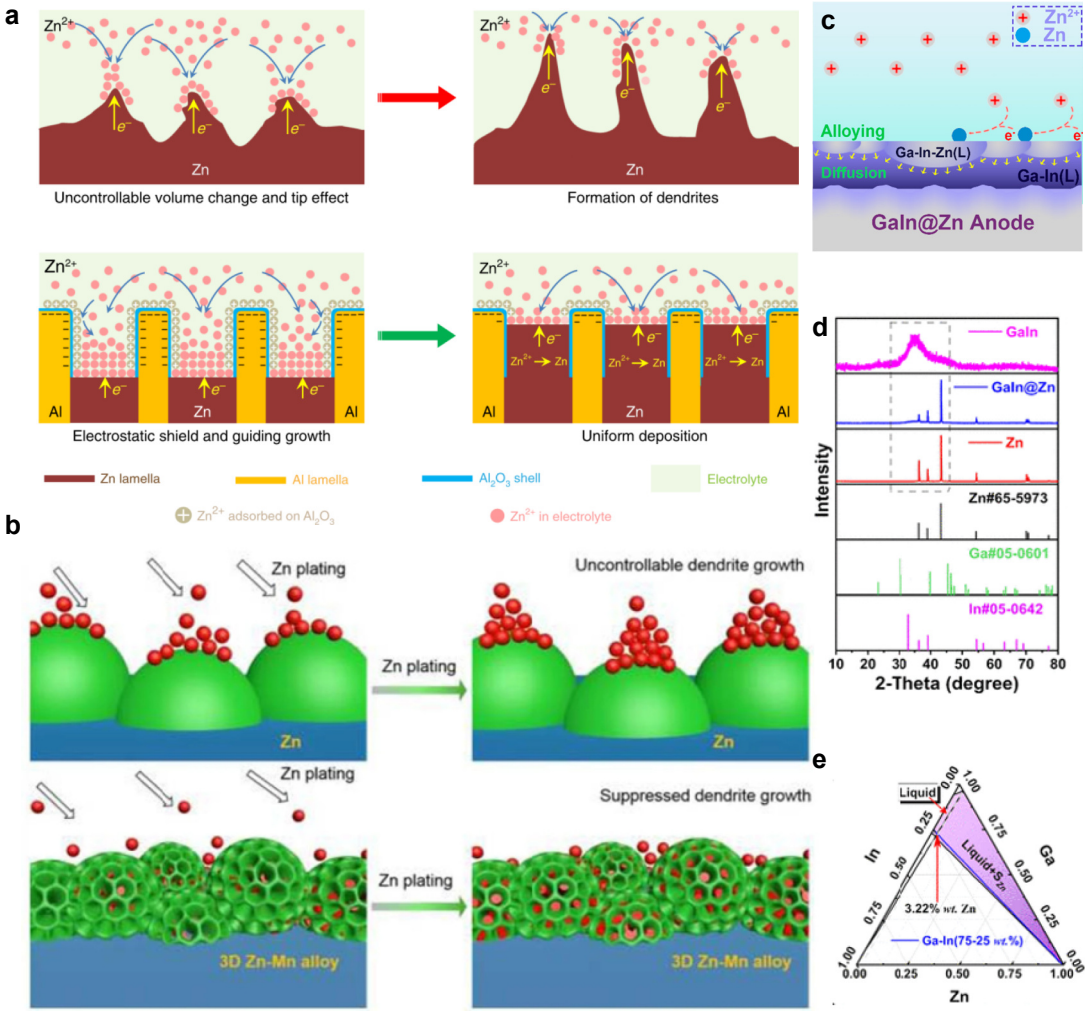

Figure 7 (a) Schematic of the eutectic strategy for dendrite inhibition. Reproduced under the CC BY 4.0 license from Ref. [141] ©2020, The Author(s). (b) Schematic of Zn plating on a Zn anode (top) and Zn–Mn anode (bottom). Reproduced under the CC BY 4.0 license from Ref. [142] ©2021, The Author(s). (c) Schematic illustration of the dendrite-free GaIn@Zn anode through an alloying-diffusion synergistic strategy. (d) XRD patterns of GaIn@Zn anode. (e) Ga-In-Zn ternary isothermal section phase diagram at 25 °C with a fixed weight ratio of 75% Ga and 25% In. Reproduced with permission from Ref. [105] ©2021, American Chemical Society.

Zn–Ni–In alloy, prepared by heat treatment, was also found to suppress HER and corrosion[143]. The high polarization of indium increases the overpotential of HER, significantly reducing both HER and corrosion.

In summary, metals can serve as heterogeneous seeds to lower the energy barrier for Zn nucleation due to their high electronic conductivity and favorable affinity with Zn metal. Various metals can promote uniform Zn deposition by increasing nucleation sites and restricting 2D diffusion of the Zn nucleus. However, the anode degradation caused by alloying reactions can lead to a sharp decrease in electrochemical performance. Therefore, liquid alloys may represent a promising strategy for the future development of alloy anodes.

4 Summary and perspectives

Given the advantages of low cost, high safety, and environmental friendliness, aqueous ZIBs are considered potential alternatives to LIBs, particularly for large-scale energy storage. However, research on the anode side remains far less mature compared to the extensive work on cathode materials aimed at enhancing energy density and cycle stability. Despite the benefits of Zn metal, including its low cost, favorable volumetric specific capacity, and abundance, several challenges must still be addressed to advance the practical application of ZIBs.

This review focuses on the key issues of dendrites, HER, and corrosion associated with the Zn metal anode. Dendritic growth in metal electrodes is primarily caused by uneven electrolyte concentration and electric field distribution at the interfaces between the current collector, zinc metal, and electrolyte. Although HER proceeds spontaneously from a thermodynamic perspective, it generally has a limited impact on battery performance due to kinetic factors. The mechanisms behind corrosion differ between the anode and cathode. On the anode side,

the rise in OH^- concentration leads to passivation, while on the cathode side, the co-intercalation of H^+ contributes to the formation of a passivation layer. While significant progress has been made in addressing these challenges, much work remains before ZIBs can be commercially viable.

We have summarized several effective strategies for modifying zinc metal anodes in Table 1. These methods, which address dendrite formation, hydrogen evolution, and corrosion in zinc metal anodes, can be broadly categorized into four groups:

1. Structural design. By enhancing ion concentration homogeneity in the electrolyte flux and ensuring a uniform electric field distribution across the current collector, 3D structures mechanically suppress dendrite growth.

2. Surface modification. The construction of buffer layers minimizes direct contact between zinc metal and the electrolyte, effectively reducing the occurrence of hydrogen evolution and passivation reactions.

3. Electrolyte modification. The addition of electrolyte additives achieves pre-desolvation or charge shielding, resulting in more uniform zinc deposition.

4. Alloying anode. The use of zinc alloy anodes introduces specialized electrode structures, leveraging alloy properties to inhibit dendrite formation and mitigate side reactions.

It is worth noting that other EESs utilizing Zn metal anodes, such as Zn-ion capacitors and Zn-air batteries, also encounter similar challenges[145,146]. The strategies discussed in this review are applicable to these systems as well.

This review aims to provide a comprehensive summary of the origins and mechanisms behind dendrite growth, hydrogen evolution, and corrosion during Zn deposition. In addition, we outline current strategies designed to mitigate these issues. This review not only enhances the understanding of recent research progress but also offers valuable insights to guide future research in the development of promising Zn-based EESs.

Acknowledgements

None.

Author contribution statement

M.-C.T. conceived the idea and supervised the project. B.Y.L., Y.T.M., J.B.M., L.K.C., Y.Z., and M.-C.T. wrote the initial paper. All the authors commented on and revised the manuscript at all stages. All the authors have approved the final manuscript.

Data availability

Not applicable.

Declaration of competing interest

All the contributing authors report no conflict of interests in this work.

Funding

The work is granted by National Natural Science

Table 1 Literature survey of previous reports of modified strategies and performance

Modified strategies	Electrolytes	Symmetric cell performance	Voltage hysteresis	References
3D carbon nanotube (CNT) framework	2 mol/L $ZnSO_4$	2 mA cm^{-2}, 2 mAh cm^{-2} for 200 h	27 mV	[83]
Nano-$CaCO_3$ coating	3 mol/L $ZnSO_4$ + 0.1 mol/L $MnSO_4$	2 mA cm^{-2}, 0.1 mAh cm^{-2} for 80 h	100 mV	[144]
Copper mesh skeleton with polyacrylamide (PAM) additive	1 mol/L $ZnSO_4$ + 0.5 mol/L Na_2SO_4 + 1 g/L PAM	2 mA cm^{-2}, 4 mAh cm^{-2} for 280 h	93.1 mV	[125]
3D nanoporous ZnO coating Zn plate	2 mol/L $ZnSO_4$	5 mA cm^{-2}, 1.25 mAh cm^{-2} for 500 h	43 mV	[89]
Lamella-nanostructured eutectic Zn–Al alloys	2 mol/L $ZnSO_4$ with the absence of O_2	0.5 mA cm^{-2} for 2000 h	~40 mV	[141]
Super-saturated electrolyte front surface	2 mol/L $ZnSO_4$	0.5 mA cm^{-2}, 0.5 mAh cm^{-2} for 3000 h	~42 mV	[90]
ZnS interphase coated Zn	1 mol/L $ZnSO_4$	2 mA cm^{-2}, 2 mAh cm^{-2} for 1100 h	~50 mV	[91]
Faceted TiO_2 coated Zn	2 mol/L $ZnSO_4$	1 mA cm^{-2}, 1 mAh cm^{-2} for 4a0h	42 mV	[108]
Directly grown vertical graphene carpets as separator	2 mol/L $ZnSO_4$	10 mA cm^{-2}, 1 mAh cm^{-2} for 600 h	73 mV	[133]
Liquid Ga–In alloy interlayer coated Zn	3 mol/L $ZnSO_4$	0.25 mA cm^{-2}, 0.05 mAh cm^{-2} for 2100 h	24 mV	[105]
3D ZnF_2 matrix coated Zn	2 mol/L $ZnSO_4$	1 mA cm^{-2}, 1 mAh cm^{-2} for 800 h	~40 mV	[93]
In situ formed Ag_3Zn coated Zn	2 mol/L $ZnSO_4$	0.25 mA cm^{-2}, 0.25 mAh cm^{-2} for 1700 h	21 mV	[92]
Zn–Mn alloys	2 mol/L $ZnSO_4$ in seawater	80 mA cm^{-2}, 16 mAh cm^{-2} for 750 h	~150 mV	[142]
Electrolyte optimization	Alg–Zn gel electrolyte	1.77 mA cm^{-2}, 0.885 mAh cm^{-2} for 270 h	90 mV	[136]
Electrolyte optimization	ionic-liquid-based Zn salt solid-state electrolyte	2 mA cm^{-2}, 1 mAh cm^{-2} for 1500 h	~75 mV	[137]

Foundation of China (Grant No. 22275114); Science and Technology Planning Project of Shenzhen Municipality (Grant No. WDZC20220817160017 003); Cross-Disciplinary Research Fund of Tsinghua Shenzhen International Graduate School (SIGS), Tsinghua University (Grant No. JC2022003); Overseas Research Cooperation Fund Research Plan of Tsinghua SIGS (Grant No. HW2023006); and Scientific Research Startup Fund of SIGS, Tsinghua University (Grant Nos. QD2021027C and QD2023001C).

Use of AI statement

None.

References

[1] Stokes, L. C., Warshaw, C. (2017). Renewable energy policy design and framing influence public support in the united states. *Nat. Energy* 2, 17107.

[2] Trancik, J. E. (2014). Renewable energy: back the renewables boom. *Nature* 507, 300–302.

[3] Lund, H. (2007). Renewable energy strategies for sustainable development. *Energy* 32, 912–919.

[4] Creutzig, F., Agoston, P., Goldschmidt, J. C., Luderer, G., Nemet, G., Pietzcker, R. C. (2017). The underestimated potential of solar energy to mitigate climate change. *Nat. Energy* 2, 17140.

[5] Obama, B. (2017). The irreversible momentum of clean energy. *Science* 355, 126–129.

[6] Etacheri, V., Marom, R., Elazari, R., Salitra, G., Aurbach, D. (2011). Challenges in the development of advanced li-ion batteries: a review. *Energy Environ. Sci.* 4, 3243–3262.

[7] Gür, T. M. (2018). Review of electrical energy storage technologies, materials and systems: challenges and prospects for large-scale grid storage. *Energy Environ. Sci.* 11, 2696–2767.

[8] Zeng, X. H., Hao, J. N., Wang, Z. J., Mao, J. F., Guo, Z. P. (2019). Recent progress and perspectives on aqueous Zn-based rechargeable batteries with mild aqueous electrolytes. *Energy Storage Mater.* 20, 410–437.

[9] Kang, K., Meng, Y. S., Bréger, J., Grey, C. P., Ceder, G. (2006). Electrodes with high power and high capacity for rechargeable lithium batteries. *Science* 311, 977–980.

[10] Tarascon, J. M., Armand, M. (2001). Issues and challenges facing rechargeable lithium batteries. *Nature* 414, 359–367.

[11] Yoshino, A. (2012). The birth of the lithium-ion battery. *Angew. Chem. Int. Ed.* 51, 5798–5800.

[12] Mei, J., Liao, T., Liang, J., Qiao, Y. X., Dou, S. X., Sun, Z. Q. (2020). Toward promising cathode catalysts for nonlithium metal-oxygen batteries. *Adv. Energy Mater.* 10, 1901997.

[13] Cabana, J., Monconduit, L., Larcher, D., Rosa Palacín, M. (2010). Beyond intercalation-based Li-ion batteries: the state of the art and challenges of electrode materials reacting through conversion reactions. *Adv. Mater.* 22, E170–E192.

[14] Schon, T. B., McAllister, B. T., Li, P. F., Seferos, D. S. (2016). The rise of organic electrode materials for energy storage. *Chem. Soc. Rev.* 45, 6345–6404.

[15] Tang, B. Y., Shan, L. T., Liang, S. Q., Zhou, J. (2019). Issues and opportunities facing aqueous zinc-ion batteries. *Energy Environ. Sci.* 12, 3288–3304.

[16] Kundu, D., Adams, B. D., Duffort, V., Vajargah, S. H., Nazar, L. F. (2016). A high-capacity and long-life aqueous rechargeable zinc battery using a metal oxide intercalation cathode. *Nat. Energy* 1, 16119.

[17] Huang, S., Zhu, J. C., Tian, J. L., Niu, Z. Q. (2019). Recent progress in the electrolytes of aqueous zinc-ion batteries. *Chem. Eur. J.* 25, 14480–14494.

[18] McBreen, J. (1994). Nickel/zinc batteries. *J. Power Sources* 51, 37–44.

[19] Liu, Y. Z., Yang, Z. H., Xie, X. E., Huang, J. H., Wen, X. (2015). Layered double oxides nano-flakes derived from layered double hydroxides: preparation, properties and application in zinc/nickel secondary batteries. *Electrochim. Acta* 185, 190–197.

[20] Smith, D. F., Gucinski, J. A. (1999). Synthetic silver oxide and mercury-free zinc electrodes for silver-zinc reserve batteries. *J. Power Sources* 80, 66–71.

[21] Mojtahedi, M., Goodarzi, M., Sharifi, B., Khaki, J. V. (2011). Effect of electrolysis condition of zinc powder production on zinc-silver oxide battery operation. *Energy Conversi. Manage.* 52, 1876–1880.

[22] Yamamoto, T., Shoji, T. (1986). Rechargeable $Zn|ZnSO_4|MnO_2$-type cells. *Inorg. Chim. Acta* 117, L27–L28.

[23] Xie, C. X., Liu, Y., Lu, W. J., Zhang, H. M., Li, X. F. (2019). Highly stable zinc-iodine single flow batteries with super high energy density for stationary energy storage. *Energy Environ. Sci.* 12, 1834–1839.

[24] Chao, D. L., Zhou, W. H., Ye, C., Zhang, Q. H., Chen, Y. G., Gu, L., Davey, K., Qiao, S. Z. (2019). An electrolytic Zn-MnO_2 battery for high-voltage and scalable energy storage. *Angew. Chem. Int. Ed.* 58, 7823–7828.

[25] Liu, Z. X., Huang, Y., Huang, Y., Yang, Q., Li, X. L., Huang, Z. D., Zhi, C. Y. (2020). Voltage issue of aqueous rechargeable metal-ion batteries. *Chem. Soc. Rev.* 49, 180–232.

[26] Xu, C. J., Li, B. H., Du, H. D., Kang, F. Y. (2012). Energetic zinc ion chemistry: the rechargeable zinc ion battery. *Angew. Chem. Int. Ed.* 51, 933–935.

[27] Zhang, Q., Luan, J. Y., Tang, Y. G., Ji, X. B., Wang, H. Y. (2020). Interfacial design of dendrite-free zinc anodes for aqueous zinc-ion batteries. *Angew. Chem. Int. Ed.* 59, 13180–13191.

[28] Han, S. D., Kim, S., Li, D. G., Petkov, V., Yoo, H. D., Phillips, P. J., Wang, H., Kim, J. J., More, K. L., Key, B., et al. (2017). Mechanism of Zn insertion into nanostructured δ-MnO_2: a nonaqueous rechargeable Zn metal battery. *Chem. Mater.* 29, 4874–4884.

[29] Wan, F., Niu, Z. Q. (2019). Design strategies for vana-

dium-based aqueous zinc-ion batteries. *Angew. Chem. Int. Ed.* 58, 16358–16367.

[30] Schmuch, R., Wagner, R., Hörpel, G., Placke, T., Winter, M. (2018). Performance and cost of materials for lithium-based rechargeable automotive batteries. *Nat. Energy* 3, 267–278.

[31] Fang, G. Z., Zhou, J., Pan, A. Q., Liang, S. Q. (2018). Recent advances in aqueous zinc-ion batteries. *ACS Energy Lett.* 3, 2480–2501.

[32] Huang, J. H., Guo, Z. W., Ma, Y. Y., Bin, D., Wang, Y. G., Xia, Y. Y. (2019). Recent progress of rechargeable batteries using mild aqueous electrolytes. *Small Methods* 3, 1800272.

[33] Boruah, B. D., Mathieson, A., Wen, B., Feldmann, S., Dose, W. M., De Volder, M. (2020). Photo-rechargeable zinc-ion batteries. *Energy Environ. Sci.* 13, 2414–2421.

[34] Winter, M., Brodd, R. J. (2004). What are batteries, fuel cells, and supercapacitors?. *Chem. Rev.* 104, 4245–4270.

[35] Wu, X. W., Xiang, Y. H., Peng, Q. J., Wu, X. S., Li, Y. H., Tang, F., Song, R. C., Liu, Z. X., He, Z. Q., Wu, X. M. (2017). Green-low-cost rechargeable aqueous zinc-ion batteries using hollow porous spinel $ZnMn_2O_4$ as the cathode material. *J. Mater. Chem. A* 5, 17990–17997.

[36] Li, Q., Wei, T. Y., Ma, K. X., Yang, G. Z., Wang, C. X. (2019). Boosting the cyclic stability of aqueous zinc-ion battery based on al-doped $V_{10}O_{24}\cdot 12H_2O$ cathode materials. *ACS Appl. Mater. Interfaces* 11, 20888–20894.

[37] Kundu, D., Oberholzer, P., Glaros, C., Bouzid, A., Tervoort, E., Pasquarello, A., Niederberger, M. (2018). Organic cathode for aqueous Zn-ion batteries: taming a unique phase evolution toward stable electrochemical cycling. *Chem. Mater.* 30, 3874–3881.

[38] Li, M., Lu, J., Chen, Z. W., Amine, K. (2018). 30 years of lithium-ion batteries. *Adv. Mater.* 30, 1800561.

[39] Fang, G. Z., Zhu, C. Y., Chen, M. H., Zhou, J., Tang, B. Y., Cao, X. X., Zheng, X. S., Pan, A. Q., Liang, S. Q. (2019). Suppressing manganese dissolution in potassium manganate with rich oxygen defects engaged high-energy-density and durable aqueous zinc-ion battery. *Adv. Funct. Mater.* 29, 1808375.

[40] Zhu, C. Y., Fang, G. Z., Liang, S. Q., Chen, Z. X., Wang, Z. Q., Ma, J. Y., Wang, H., Tang, B. Y., Zheng, X. S., Zhou, J. (2020). Electrochemically induced cationic defect in MnO intercalation cathode for aqueous zinc-ion battery. *Energy Storage Mater.* 24, 394–401.

[41] Yang, Y. Q., Tang, Y., Fang, G. Z., Shan, L. T., Guo, J. S., Zhang, W. Y., Wang, C., Wang, L. B., Zhou, J., Liang, S. Q. (2018). Li^+ intercalated $V_2O_5\cdot nH_2O$ with enlarged layer spacing and fast ion diffusion as an aqueous zinc-ion battery cathode. *Energy Environ. Sci.* 11, 3157–3162.

[42] Tang, B. Y., Fang, G. Z., Zhou, J., Wang, L. B., Lei, Y. P., Wang, C., Lin, T. Q., Tang, Y., Liang, S. Q. (2018). Potassium vanadates with stable structure and fast ion diffusion channel as cathode for rechargeable aqueous zinc-ion batteries. *Nano Energy* 51, 579–587.

[43] Liu, C. F., Neale, Z., Zheng, J. Q., Jia, X. X., Huang, J. J., Yan, M. Y., Tian, M., Wang, M. S., Yang, J. H., Cao, G. Z. (2019). Expanded hydrated vanadate for high-performance aqueous zinc-ion batteries. *Energy Environ. Sci.* 12, 2273–2285.

[44] Zhang, L. Y., Chen, L., Zhou, X. F., Liu, Z. P. (2015). Morphology-dependent electrochemical performance of zinc hexacyanoferrate cathode for zinc-ion battery. *Sci. Rep.* 5, 18263.

[45] Zhang, L. Y., Chen, L., Zhou, X. F., Liu, Z. P. (2015). Towards high-voltage aqueous metal-ion batteries beyond 1.5 V: the zinc/zinc hexacyanoferrate system. *Adv. Energy Mater.* 5, 1400930.

[46] Zhao, Q., Huang, W. W., Luo, Z. Q., Liu, L. J., Lu, Y., Li, Y. X., Li, L., Hu, J. Y., Ma, H., Chen, J. (2018). High-capacity aqueous zinc batteries using sustainable quinone electrodes. *Sci. Adv.* 4, eaao1761.

[47] Zhao, Z. Q., Fan, X. Y., Ding, J., Hu, W. B., Zhong, C., Lu, J. (2019). Challenges in zinc electrodes for alkaline zinc-air batteries: obstacles to commercialization. *ACS Energy Lett.* 4, 2259–2270.

[48] Zhang, R., Chen, X. R., Chen, X., Cheng, X. B., Zhang, X. Q., Yan, C., Zhang, Q. (2017). Lithiophilic sites in doped graphene guide uniform lithium nucleation for dendrite-free lithium metal anodes. *Angew. Chem. Int. Ed.* 56, 7764–7768.

[49] Zeng, Y. X., Zhang, X. Y., Meng, Y., Yu, M. H., Yi, J. N., Wu, Y. Q., Lu, X. H., Tong, Y. X. (2017). Achieving ultrahigh energy density and long durability in a flexible rechargeable quasi-solid-state Zn-MnO_2 battery. *Adv. Mater.* 29, 1700274.

[50] Yi, Z. H., Chen, G. Y., Hou, F., Wang, L. Q., Liang, J. (2021). Strategies for the stabilization of Zn metal anodes for Zn-ion batteries. *Adv. Energy Mater.* 11, 2003065.

[51] Mainar, A. R., Leonet, O., Bengoechea, M., Boyano, I., de Meatza, I., Kvasha, A., Guerfi, A., Alberto Blázquez, J. (2016). Alkaline aqueous electrolytes for secondary zinc-air batteries: an overview. *Int. J. Energy Res.* 40, 1032–1049.

[52] Lu, W. J., Xie, C. X., Zhang, H. M., Li, X. F. (2018). Inhibition of zinc dendrite growth in zinc-based batteries. *ChemSusChem* 11, 3996–4006.

[53] Yufit, V., Tariq, F., Eastwood, D. S., Biton, M., Wu, B., Lee, P. D., Brandon, N. P. (2019). *Operando* visualization and multi-scale tomography studies of dendrite formation and dissolution in zinc batteries. *Joule* 3, 485–502.

[54] Konarov, A., Voronina, N., Jo, J. H., Bakenov, Z., Sun, Y. K., Myung, S. T. (2018). Present and future perspective on electrode materials for rechargeable zinc-ion batteries. *ACS Energy Lett.* 3, 2620–2640.

[55] Zhao, Z. M., Zhao, J. W., Hu, Z. L., Li, J. D., Li, J. J., Zhang, Y. J., Wang, C., Cui, G. L. (2019). Long-life and deeply rechargeable aqueous Zn anodes enabled by a multifunctional brightener-inspired interphase. *Energy Environ. Sci.* 12, 1938–1949.

[56] Al-Hinai, A. T., Al-Hinai, M. H., Dutta, J. (2014). Application of E_h-pH diagram for room temperature precipitation of zinc stannate microcubes in an aqueous media. *Mater. Res. Bull.* 49, 645–650.

[57] Chao, D. L., Zhou, W. H., Xie, F. X., Ye, C., Li, H., Jaroniec, M., Qiao, S. Z. (2020). Roadmap for advanced aqueous batteries: from design of materials to applications. *Sci. Adv.* 6, eaba4098.

[58] Blanc, L. E., Kundu, D., Nazar, L. F. (2020). Scientific challenges for the implementation of Zn-ion batteries. *Joule* 4, 771–799.

[59] Lee, B. S., Cui, S., Xing, X., Liu, H. D., Yue, X. J., Petrova, V., Lim, H. D., Chen, R. K., Liu, P. (2018). Dendrite suppression membranes for rechargeable zinc batteries. *ACS Appl. Mater. Interfaces* 10, 38928–38935.

[60] Li, C. P., Xie, X. S., Liang, S. Q., Zhou, J. (2020). Issues and future perspective on zinc metal anode for rechargeable aqueous zinc-ion batteries. *Energy Environ. Mater.* 3, 146–159.

[61] Yang, Q., Bang, G. J., Guo, Y., Liu, Z. X., Yon, B. X., Wang, D. H., Huang, Z. D., Li, X. L., Fan, J., Zhi, C. Y. (2019). Do zinc dendrites exist in neutral zinc batteries: a developed electrohealing strategy to *in situ* rescue in-service batteries. *Adv. Mater.* 31, 1903778.

[62] Zhao, J. W., Zhang, J., Yang, W. H., Chen, B. B., Zhao, Z. M., Qiu, H. Y., Dong, S. M., Zhou, X. H., Cui, G. L., Chen, L. Q. (2019). "Water-in-deep eutectic solvent" electrolytes enable zinc metal anodes for rechargeable aqueous batteries. *Nano Energy* 57, 625–634.

[63] González, M. A., Trócoli, R., Pavlovic, I., Barriga, C., La Mantia, F. (2016). Layered double hydroxides as a suitable substrate to improve the efficiency of Zn anode in neutral pH Zn-ion batteries. *Electrochem. Commun.* 68, 1–4.

[64] Krężel, A., Maret, W. (2016). The biological inorganic chemistry of zinc ions. *Arch. Biochem. Biophys.* 611, 3–19.

[65] Trócoli, R., La Mantia, F. (2015). An aqueous zinc-ion battery based on copper hexacyanoferrate. *ChemSusChem* 8, 481–485.

[66] Li, Y. G., Dai, H. J. (2014). Recent advances in zinc-air batteries. *Chem. Soc. Rev.* 43, 5257–5275.

[67] Alfaruqi, M. H., Islam, S., Mathew, V., Song, J. J., Kim, S., Tung, D. P., Jo, J., Kim, S., Baboo, J. P., Xiu, Z. L., et al. (2017). Ambient redox synthesis of vanadium-doped manganese dioxide nanoparticles and their enhanced zinc storage properties. *Appl. Surf. Sci.* 404, 435–442.

[68] Cho, Y. D., Fey, G. T. K. (2008). Surface treatment of zinc anodes to improve discharge capacity and suppress hydrogen gas evolution. *J. Power Sources* 184, 610–616.

[69] Ibrahim, M. A. M. (2000). Improving the throwing power of acidic zinc sulfate electroplating baths. *J. Chem. Technol. Biotechnol.* 75, 745–755.

[70] Kühne, H. M., Schefold, J. (1990). Tafel plots from illuminated photoelectrodes: a new insight into charge transfer mechanism. *J. Electrochem. Soc.* 137, 568–575.

[71] Miles, M. H., Kissel, G., Lu, P. W. T., Srinivasan, S. (1976). Effect of temperature on electrode kinetic parameters for hydrogen and oxygen evolution reactions on nickel electrodes in alkaline solutions. *J. Electrochem. Soc.* 123, 332–336.

[72] Dong, H. X., Lei, T., He, Y. H., Xu, N. P., Huang, B. Y., Liu, C. T. (2011). Electrochemical performance of porous Ni_3Al electrodes for hydrogen evolution reaction. *Int. J. Hydrogen Energy* 36, 12112–12120.

[73] Wippermann, K., Schultze, J. W., Kessel, R., Penninger, J. (1991). The inhibition of zinc corrosion by bisaminotriazole and other triazole derivatives. *Corros. Sci.* 32, 205–230.

[74] Hoang, T. K. A., The Nam Long Doan, Sun, K. E. K., Chen, P. (2015). Corrosion chemistry and protection of zinc & zinc alloys by polymer-containing materials for potential use in rechargeable aqueous batteries. *RSC Adv.* 5, 41677–41691.

[75] Li, H. F., Xu, C. J., Han, C. P., Chen, Y. Y., Wei, C. G., Li, B. H., Kang, F. Y. (2015). Enhancement on cycle performance of Zn anodes by activated carbon modification for neutral rechargeable zinc ion batteries. *J. Electrochem. Soc.* 162, A1439–A1444.

[76] Pan, H. L., Ellis, J. F., Li, X. L., Nie, Z. M., Chang, H. J., Reed, D. (2019). Electrolyte effect on the electrochemical performance of mild aqueous zinc-electrolytic manganese dioxide batteries. *ACS Appl. Mater. Interfaces* 11, 37524–37530.

[77] Tie, Z. W., Liu, L. J., Deng, S. Z., Zhao, D. B., Niu, Z. Q. (2020). Proton insertion chemistry of a zinc-organic battery. *Angew. Chem. Int. Ed.* 59, 4920–4924.

[78] Oberholzer, P., Tervoort, E., Bouzid, A., Pasquarello, A., Kundu, D. (2019). Oxide versus nonoxide cathode materials for aqueous Zn batteries: an insight into the charge storage mechanism and consequences thereof. *ACS Appl. Mater. Interfaces* 11, 674–682.

[79] Huang, J. H., Wang, Z., Hou, M. Y., Dong, X. L., Liu, Y., Wang, Y. G., Xia, Y. Y. (2018). Polyaniline-intercalated manganese dioxide nanolayers as a high-performance cathode material for an aqueous zinc-ion battery. *Nat. Commun.* 9, 2906.

[80] Liu, W. B., Dong, L. B., Jiang, B. Z., Huang, Y. F., Wang, X. L., Xu, C. J., Kang, Z., Mou, J., Kang, F. Y. (2019). Layered vanadium oxides with proton and zinc ion insertion for zinc ion batteries. *Electrochim. Acta* 320, 134565.

[81] Guo, W. B., Cong, Z. F., Guo, Z. H., Chang, C. Y., Liang, X. Q., Liu, Y. D., Hu, W. G., Pu, X. (2020). Dendrite-free Zn anode with dual channel 3D porous frameworks for rechargeable Zn batteries. *Energy Storage Mater.* 30, 104–112.

[82] Lee, J. H., Kim, R., Kim, S., Heo, J., Kwon, H., Yang, J. H., Kim, H. T. (2020). Dendrite-free Zn electrodeposition triggered by interatomic orbital hybridization of Zn and single vacancy carbon defects for aqueous Zn-based flow batteries. *Energy Environ. Sci.* 13, 2839–2848.

[83] Zeng, Y. X., Zhang, X. Y., Qin, R. F., Liu, X. Q., Fang, P. P., Zheng, D. Z., Tong, Y. X., Lu, X. H. (2019). Dendrite-free zinc deposition induced by multifunctional CNT frameworks for stable flexible Zn-ion batteries. *Adv. Mater.* 31, 1903676.

[84] Xue, P., Guo, C., Li, L., Li, H. P., Luo, D., Tan, L. C., Chen, Z. W. (2022). A MOF-derivative decorated hierar-

chical porous host enabling ultrahigh rates and superior long-term cycling of dendrite-free Zn metal anodes. *Adv. Mater.* 34, 2110047.

[85] Jin, X. T., Song, L., Dai, C. L., Xiao, Y. K., Han, Y. Y., Li, X. Y., Wang, Y., Zhang, J. T., Zhao, Y., Zhang, Z. P., et al. (2022). A flexible aqueous zinc-iodine microbattery with unprecedented energy density. *Adv. Mater.* 34, 2109450.

[86] Wang, L. P., Li, N. W., Wang, T. S., Yin, Y. X., Guo, Y. G., Wang, C. R. (2017). Conductive graphite fiber as a stable host for zinc metal anodes. *Electrochim. Acta* 244, 172–177.

[87] Kang, Z., Wu, C. L., Dong, L. B., Liu, W. B., Mou, J., Zhang, J. W., Chang, Z. W., Jiang, B. Z., Wang, G. X., Kang, F. Y., et al. (2019). 3D porous copper skeleton supported zinc anode toward high capacity and long cycle life zinc ion batteries. *ACS Sustain. Chem. Eng.* 7, 3364–3371.

[88] Cao, Q. H., Gao, Y., Pu, J., Zhao, X., Wang, Y. X., Chen, J. P., Guan, C. (2023). Gradient design of imprinted anode for stable Zn-ion batteries. *Nat. Commun.* 14, 641.

[89] Xie, X. S., Liang, S. Q., Gao, J. W., Guo, S., Guo, J. B., Wang, C., Xu, G. Y., Wu, X. W., Chen, G., Zhou, J. (2020). Manipulating the ion-transfer kinetics and interface stability for high-performance zinc metal anodes. *Energy Environ. Sci.* 13, 503–510.

[90] Yang, H. J., Chang, Z., Qiao, Y., Deng, H., Mu, X. W., He, P., Zhou, H. S. (2020). Constructing a super-saturated electrolyte front surface for stable rechargeable aqueous zinc batteries. *Angew. Chem. Int. Ed.* 59, 9377–9381.

[91] Hao, J. N., Li, B., Li, X. L., Zeng, X. H., Zhang, S. L., Yang, F. H., Liu, S. L., Li, D., Wu, C., Guo, Z. P. (2020). An in-depth study of Zn metal surface chemistry for advanced aqueous Zn-ion batteries. *Adv. Mater.* 32, 2003021.

[92] Wang, Y. Y., Chen, Y. J., Liu, W., Ni, X. Y., Qing, P., Zhao, Q. W., Wei, W. F., Ji, X. B., Ma, J. M., Chen, L. B. (2021). Uniform and dendrite-free zinc deposition enabled by *in situ* formed $AgZn_3$ for the zinc metal anode. *J. Mater. Chem. A* 9, 8452–8461.

[93] Yang, Y., Liu, C. Y., Lv, Z. H., Yang, H., Zhang, Y. F., Ye, M. H., Chen, L. B., Zhao, J. B., Li, C. C. (2021). Synergistic manipulation of Zn^{2+} ion flux and desolvation effect enabled by anodic growth of a 3D ZnF_2 matrix for long-lifespan and dendrite-free Zn metal anodes. *Adv. Mater.* 33, 2007388.

[94] Budevski, E., Staikov, G., Lorenz, W. J. (2000). Electrocrystallization: nucleation and growth phenomena. *Electrochim. Acta* 45, 2559–2574.

[95] Xie, F. X., Li, H., Wang, X. S., Zhi, X., Chao, D. L., Davey, K., Qiao, S. Z. (2021). Mechanism for zincophilic sites on zinc-metal anode hosts in aqueous batteries. *Adv. Energy Mater.* 11, 2003419.

[96] Li, B., Yang, K. Y., Ma, J. B., Shi, P. R., Chen, L. K., Chen, C. M., Hong, X., Cheng, X., Tang, M. C., He, Y. B., et al. (2022). Multicomponent copper-zinc alloy layer enabling ultra-stable zinc metal anode of aqueous Zn-ion battery. *Angew. Chem. Int. Ed.* 61, e202212587.

[97] Yu, H. M., Chen, Y. J., Wei, W. F., Ji, X. B., Chen, L. B. (2022). A functional organic zinc-chelate formation with nanoscaled granular structure enabling long-term and dendrite-free Zn anodes. *ACS Nano* 16, 9736–9747.

[98] Zhang, S. J., Ye, J. J., Ao, H. S., Zhang, M. Y., Li, X. L., Xu, Z. B., Hou, Z. G., Qian, Y. T. (2023). *In-situ* formation of hierarchical solid-electrolyte interphase for ultra-long cycling of aqueous zinc-ion batteries. *Nano Res.* 16, 449–457.

[99] Zhou, M., Guo, S., Fang, G. Z., Sun, H. M., Cao, X. X., Zhou, J., Pan, A. Q., Liang, S. Q. (2021). Suppressing by-product via stratified adsorption effect to assist highly reversible zinc anode in aqueous electrolyte. *J. Energy Chem.* 55, 549–556.

[100] Zhou, J. H., Xie, M., Wu, F., Mei, Y., Hao, Y. T., Huang, R. L., Wei, G. L., Liu, A. N., Li, L., Chen, R. J. (2021). Ultrathin surface coating of nitrogen-doped graphene enables stable zinc anodes for aqueous zinc-ion batteries. *Adv. Mater.* 33, 2101649.

[101] Yin, Y. B., Wang, S. N., Zhang, Q., Song, Y., Chang, N. N., Pan, Y. W., Zhang, H. M., Li, X. F. (2020). Dendrite-free zinc deposition induced by tin-modified multifunctional 3D host for stable zinc-based flow battery. *Adv. Mater.* 32, 1906803.

[102] Novotny, P. M. (2007). Toughness index for alloy comparisons. *Adv. Mater. Processes* 165, 29–31.

[103] Toulfatzis, A. I., Pantazopoulos, G. A., Paipetis, A. S. (2014). Fracture behavior and characterization of lead-free brass alloys for machining applications. *J. Mater. Eng. Perform.* 23, 3193–3206.

[104] Meng, H., Ran, Q., Dai, T. Y., Shi, H., Zeng, S. P., Zhu, Y. F., Wen, Z., Zhang, W., Lang, X. Y., Zheng, W. T., et al. (2022). Surface-alloyed nanoporous zinc as reversible and stable anodes for high-performance aqueous zinc-ion battery. *Nano-Micro Lett.* 14, 128.

[105] Liu, C., Luo, Z., Deng, W. T., Wei, W. F., Chen, L. B., Pan, A. Q., Ma, J. M., Wang, C. W., Zhu, L. M., Xie, L. L., et al. (2021). Liquid alloy interlayer for aqueous zinc-ion battery. *ACS Energy Lett.* 6, 675–683.

[106] Zheng, J. X., Huang, Z. H., Zeng, Y., Liu, W. Q., Wei, B. B., Qi, Z. B., Wang, Z. C., Xia, C., Liang, H. F. (2022). Electrostatic shielding regulation of magnetron sputtered Al-based alloy protective coatings enables highly reversible zinc anodes. *Nano Lett.* 22, 1017–1023.

[107] Xu, F., Qu, C. Z., Lu, Q. Q., Meng, J. S., Zhang, X. H., Xu, X. S., Qiu, Y. Q., Ding, B. C., Yang, J. Y., Cao, F. R., et al. (2022). Atomic Sn-enabled high-utilization, large-capacity, and long-life Na anode. *Sci. Adv.* 8, eabm7489.

[108] Zhang, Q., Luan, J. Y., Huang, X. B., Wang, Q., Sun, D., Tang, Y. G., Ji, X. B., Wang, H. Y. (2020). Revealing the role of crystal orientation of protective layers for stable zinc anode. *Nat. Commun.* 11, 3961.

[109] Zheng, J. X., Zhao, Q., Tang, T., Yin, J. E., Quilty, C. D., Renderos, G. D., Liu, X. T., Deng, Y., Wang, L., Bock, D. C., et al. (2019). Reversible epitaxial electrodeposition of metals in battery anodes. *Science* 366, 645–648.

[110] Xie, C. L., Liu, S. F., Yang, Z. F., Ji, H. M., Zhou, S. H., Wu, H., Hu, C., Tang, Y. G., Ji, X. B., Zhang, Q., et al. (2023). Discovering the intrinsic causes of dendrite formation in zinc metal anodes: lattice defects and residual stress. *Angew. Chem. Int. Ed.* 62, e202218612.

[111] Xia, A. L., Pu, X. M., Tao, Y. Y., Liu, H. M., Wang, Y. G. (2019). Graphene oxide spontaneous reduction and self-assembly on the zinc metal surface enabling a dendrite-free anode for long-life zinc rechargeable aqueous batteries. *Appl. Surf. Sci.* 481, 852–859.

[112] Gao, S. S., Zhang, Z., Mao, F. F., Liu, P. G., Zhou, Z. (2023). Advances and strategies of electrolyte regulation in Zn-ion batteries. *Mater. Chem. Front.* 7, 3232–3258.

[113] Olbasa, B. W., Fenta, F. W., Chiu, S. F., Tsai, M. C., Huang, C. J., Jote, B. A., Beyene, T. T., Liao, Y. F., Wang, C. H., Su, W. N., et al. (2020). High-rate and long-cycle stability with a dendrite-free zinc anode in an aqueous Zn-ion battery using concentrated electrolytes. *ACS Appl. Energy Mater.* 3, 4499–4508.

[114] Zhang, N., Cheng, F. Y., Liu, J. X., Wang, L. B., Long, X. H., Liu, X. S., Li, F. J., Chen, J. (2017). Rechargeable aqueous zinc-manganese dioxide batteries with high energy and power densities. *Nat. Commun.* 8, 405.

[115] Chae, M. S., Heo, J. W., Lim, S. C., Hong, S. T. (2016). Electrochemical zinc-ion intercalation properties and crystal structures of $ZnMo_6S_8$ and $Zn_2Mo_6S_8$ chevrel phases in aqueous electrolytes. *Inorg. Chem.* 55, 3294–3301.

[116] Hao, J. W., Mou, J., Zhang, J. W., Dong, L. B., Liu, W. B., Xu, C. J., Kang, F. Y. (2018). Electrochemically induced spinel-layered phase transition of Mn_3O_4 in high performance neutral aqueous rechargeable zinc battery. *Electrochim. Acta* 259, 170–178.

[117] Zhou, J., Shan, L. T., Wu, Z. X., Guo, X., Fang, G. Z., Liang, S. Q. (2018). Investigation of V_2O_5 as a low-cost rechargeable aqueous zinc ion battery cathode. *Chem. Commun.* 54, 4457–4460.

[118] Yan, C., Li, H. R., Chen, X., Zhang, X. Q., Cheng, X. B., Xu, R., Huang, J. Q., Zhang, Q. (2019). Regulating the inner helmholtz plane for stable solid electrolyte interphase on lithium metal anodes. *J. Am. Chem. Soc.* 141, 9422–9429.

[119] Zhang, Q., Xia, K. X., Ma, Y. L., Lu, Y., Li, L., Liang, J., Chou, S. L., Chen, J. (2021). Chaotropic anion and fast-kinetics cathode enabling low-temperature aqueous Zn batteries. *ACS Energy Lett.* 6, 2704–2712.2.

[120] Wang, F., Borodin, O., Gao, T., Fan, X. L., Sun, W., Han, F. D., Faraone, A., Dura, J. A., Xu, K., Wang, C. S. (2018). Highly reversible zinc metal anode for aqueous batteries. *Nat. Mater.* 17, 543–549.

[121] Xu, M. Y., Zhu, T., Zhang, J. Z. H. (2019). Molecular dynamics simulation of zinc ion in water with an ab initio based neural network potential. *J. Phys. Chem. A* 123, 6587–6595.

[122] Sun, K. E. K., Hoang, T. K. A., The Nam Long Doan, Yu, Y., Zhu, X., Tian, Y., Chen, P. (2017). Suppression of dendrite formation and corrosion on zinc anode of secondary aqueous batteries. *ACS Appl. Mater. Interfaces* 9, 9681–9687.

[123] Lin, C. Y., Yang, X. H., Xiong, P. X., Lin, H., He, L. J., Yao, Q., Wei, M. D., Qian, Q. R., Chen, Q. H., Zeng, L. X. (2022). High-rate, large capacity, and long life dendrite-free Zn metal anode enabled by trifunctional electrolyte additive with a wide temperature range. *Adv. Sci.* 9, 2201433.

[124] Geng, L. S., Meng, J. S., Wang, X. P., Han, C. H., Han, K., Xiao, Z. T., Huang, M., Xu, P., Zhang, L., Zhou, L., et al. (2022). Eutectic electrolyte with unique solvation structure for high-performance zinc-ion batteries. *Angew. Chem. Int. Ed.* 61, e202206717.

[125] Zhang, Q., Luan, J. Y., Fu, L., Wu, S. G., Tang, Y. G., Ji, X. B., Wang, H. Y. (2019). The three-dimensional dendrite-free zinc anode on a copper mesh with a zinc-oriented polyacrylamide electrolyte additive. *Angew. Chem. Int. Ed.* 58, 15841–15847.

[126] Liu, P. G., Guo, J., Chen, X. Y., Wang, T., Huang, Y. P., Gao, S. S., Wang, T., Wu, D. L., Liu, K. Y. (2024). A zincophilic molecular brush for a dendrite-free, corrosion-resistant, zinc metal anode with a long life cycle. *Nano Res.* 17, 390–396.

[127] Shi, J. Q., Sun, T. J., Bao, J. Q., Zheng, S. B., Du, H. H., Li, L., Yuan, X. M., Ma, T., Tao, Z. L. (2021). "Water-in-deep eutectic solvent" electrolytes for high-performance aqueous Zn-ion batteries. *Adv. Funct. Mater.* 31, 2102035.

[128] Xu, W. N., Zhao, K. N., Huo, W. C., Wang, Y. Z., Yao, G., Gu, X., Cheng, H. W., Mai, L. Q., Hu, C. G., Wang, X. D. (2019). Diethyl ether as self-healing electrolyte additive enabled long-life rechargeable aqueous zinc ion batteries. *Nano Energy* 62, 275–281.

[129] Ding, F., Xu, W., Graff, G. L., Zhang, J., Sushko, M. L., Chen, X. L., Shao, Y. Y., Engelhard, M. H., Nie, Z. M., Xiao, J. L., et al. (2013). Dendrite-free lithium deposition via self-healing electrostatic shield mechanism. *J. Am. Chem. Soc.* 135, 4450–4456.

[130] Soundharrajan, V., Sambandam, B., Kim, S., Islam, S., Jo, J., Kim, S., Mathew, V., Sun, Y. K., Kim, J. (2020). The dominant role of Mn^{2+} additive on the electrochemical reaction in $ZnMn_2O_4$ cathode for aqueous zinc-ion batteries. *Energy Storage Mater.* 28, 407–417.

[131] Wan, F., Zhang, L. L., Dai, X., Wang, X. Y., Niu, Z. Q., Chen, J. (2018). Aqueous rechargeable zinc/sodium vanadate batteries with enhanced performance from simultaneous insertion of dual carriers. *Nat. Commun.* 9, 1656.

[132] Qiu, M. J., Sun, P., Han, K., Pang, Z. J., Du, J., Li, J. L., Chen, J., Wang, Z. L., Mai, W. J. (2023). Tailoring water structure with high-tetrahedral-entropy for antifreezing electrolytes and energy storage at −80 °C. *Nat. Commun.* 14, 601.

[133] Li, C., Sun, Z. T., Yang, T., Yu, L. H., Wei, N., Tian, Z. N., Cai, J. S., Lv, J. Z., Shao, Y. L., Rümmeli, M. H., et al. (2020). Directly grown vertical graphene carpets as janus separators toward stabilized Zn metal anodes. *Adv. Mater.* 32, 2003425.

[134] Bruce, P. G., Freunberger, S. A., Hardwick, L. J., Tarascon, J. M. (2012). Li-O_2 and Li-S batteries with high

energy storage. *Nat. Mater.* 11, 19–29.

[135] Xia, M. T., Fu, H. W., Lin, K. R., Rao, A. M., Cha, L. M., Liu, H., Zhou, J., Wang, C. X., Lu, B. A. (2024). Hydrogen-bond regulation in organic/aqueous hybrid electrolyte for safe and high-voltage K-ion batteries. *Energy Environ. Sci.* 17, 1255–1265.

[136] Tang, Y., Liu, C. X., Zhu, H. R., Xie, X. S., Gao, J. W., Deng, C. B., Han, M. M., Liang, S. Q., Zhou, J. (2020). Ion-confinement effect enabled by gel electrolyte for highly reversible dendrite-free zinc metal anode. *Energy Storage Mater.* 27, 109–116.

[137] Ma, L. T., Chen, S. M., Li, N., Liu, Z. X., Tang, Z. J., Zapien, J. A., Chen, S. M., Fan, J., Zhi, C. Y. (2020). Hydrogen-free and dendrite-free all-solid-state Zn-ion batteries. *Adv. Mater.* 32, 1908121.

[138] Cai, Z., Ou, Y. T., Wang, J. D., Xiao, R., Fu, L., Yuan, Z., Zhan, R. M., Sun, Y. M. (2020). Chemically resistant Cu-Zn/Zn composite anode for long cycling aqueous batteries. *Energy Storage Mater.* 27, 205–211.

[139] Zhou, J. H., Wu, F., Mei, Y., Hao, Y. T., Li, L., Xie, M., Chen, R. J. (2022). Establishing thermal infusion method for stable zinc metal anodes in aqueous zinc-ion batteries. *Adv. Mater.* 34, 2200782.

[140] Fayette, M., Chang, H. J., Rodríguez-Pérez, I. A., Li, X. L., Reed, D. (2020). Electrodeposited zinc-based films as anodes for aqueous zinc batteries. *ACS Appl. Mater. Interfaces* 12, 42763–42772.

[141] Wang, S. B., Ran, Q., Yao, R. Q., Shi, H., Wen, Z., Zhao, M., Lang, X. Y., Jiang, Q. (2020). Lamella-nanostructured eutectic zinc-aluminum alloys as reversible and dendrite-free anodes for aqueous rechargeable batteries. *Nat. Commun.* 11, 1634.

[142] Tian, H. J., Li, Z., Feng, G. X., Yang, Z. Z., Fox, D., Wang, M. Y., Zhou, H., Zhai, L., Kushima, A., Du, Y. G., et al. (2021). Stable, high-performance, dendrite-free, seawater-based aqueous batteries. *Nat. Commun.* 12, 237.

[143] Lee, C. W., Sathiyanarayanan, K., Eom, S. W., Yun, M. S. (2006). Novel alloys to improve the electrochemical behavior of zinc anodes for zinc/air battery. *J. Power Sources* 160, 1436–1441.

[144] Kang, L., Cui, M., Jiang, F., Gao, Y., Luo, H., Liu, J., Liang, W., Zhi, C. (2018). Nanoporous $CaCO_3$ coatings enabled uniform Zn stripping/plating for long-life zinc rechargeable aqueous batteries. *Adv. Energy Mater.* 8, 1801090.

[145] Zhao, J. W., Li, J. J., Han, P. X., Cui, G. L. (2017). An aqueous Zn-ion capacitor (*in Chinese*). *J. Electrochem.* 23, 581–585.

[146] Wang, Y. J., Cao, Q. H., Guan, C., Cheng, C. W. (2020). Recent advances on self-supported arrayed bifunctional oxygen electrocatalysts for flexible solid-state Zn-Air batteries. *Small* 16, 2002902.